

International Journal of Modern Physics D
© World Scientific Publishing Company

Radio Pulsars: The Neutron Star Population & Fundamental Physics

VICTORIA M. KASPI

*Department of Physics, McGill University, Rutherford Physics Building
McGill Space Institute
Montreal, Quebec H3W 2C4, Canada
vkaspi@physics.mcgill.ca*

MICHAEL KRAMER

*Max-Planck-Institut für Radioastronomie, Auf dem Hügel 69, 53121 Bonn, Germany
Jodrell Bank Centre for Astrophysics, University of Manchester, Alan-Turing-Building,
Manchester M13 9PL, UK
mkramer@mpifr.de*

Received Day Month Year

Revised Day Month Year

Radio pulsars are unique laboratories for a wide range of physics and astrophysics. Understanding how they are created, how they evolve and where we find them in the Galaxy, with or without binary companions, is highly constraining of theories of stellar and binary evolution. Pulsars' relationship with a recently discovered variety of apparently different classes of neutron stars is an interesting modern astrophysical puzzle which we consider in Part I of this review. Radio pulsars are also famous for allowing us to probe the laws of nature at a fundamental level. They act as precise cosmic clocks and, when in a binary system with a companion star, provide indispensable venues for precision tests of gravity. The different applications of radio pulsars for fundamental physics will be discussed in Part II. We finish by making mention of the newly discovered class of astrophysical objects, the Fast Radio Bursts, which may or may not be related to radio pulsars or neutron stars, but which were discovered in observations of the latter.

Keywords: Pulsars; Neutron Stars; magnetars; experimental test of gravitational theories

PACS numbers: 97.60.Gb, 97.60.Jd, 04.80.Cc

1. Introduction

The discovery of evidence for the neutron by Chadwick in 1932 was a major milestone in physics,¹ and was surely discussed with great excitement at the 1933 Solvay Conference titled “Structure et propriétés des noyaux atomiques.” That same year, two now-famous astronomers, Walter Baade and Fritz Zwicky, suggested the existence of *neutron stars*, which they argued were formed when a massive star collapses in a “super-nova”.² They argued that such a star “may possess a very small radius and an extremely high density.” It took over 3 decades for this seemingly prophetic

prediction to be confirmed: in 1967^a then-graduate student Jocelyn Bell and her PhD supervisor Antony Hewish detected the first radio pulsar,³ and Shklovksy suggested that the X-ray source Sco X-1 was an accreting neutron star.⁴ The focus of this paper is on the former discovery, now a class of celestial objects of which over 2300 are known in our Galaxy (although the accreting variety will be mentioned in §3). Though radio pulsars were compellingly identified as neutron stars not long after their discovery,^{5,6} the radio emission was unexpected, prompting the noted physicist and astronomer John Wheeler to remark his surprise that neutron stars come equipped with a handle and a bell^b. Though the origin of the radio emission is not well understood today, it has nevertheless served as a valuable beacon with which we have learned vast amounts about the neutron star phenomenon. Using this beacon as a tool also provides us with unique laboratories to study fundamental physics. In this first part of this contribution, we will review the diversity in the “neutron star zoo,” before we discuss their applications for understanding the laws of nature, in particular gravity, in the second part.

Part I: The Different Manifestations of Neutron Stars

2. Radio Pulsars

Radio pulsars are rapidly rotating, highly magnetized neutron stars whose magnetic and rotation axes are significantly misaligned. It is believed that beams of radio waves emanate from the magnetic pole region and are observed as pulsations to fortuitously located observers, with one pulse per rotation. In some cases, two pulses per rotation may be visible if the source’s magnetic and rotation axes are nearly orthogonal. Pulsations are believed to be produced, and occasionally are observed, across the full electromagnetic spectrum (see §2.1), however the vast majority of known pulsars are observed exclusively in the radio band. The known pulsar population, currently consisting of over 2300 sources with numbers constantly increasing thanks to ongoing radio pulsar surveys,^{8–10} is largely confined to the Galactic Plane, with a e^{-1} thickness of ~ 100 pc.¹¹ However, the pulsar scale height appears to increase with source age. This is presumably because pulsars are high velocity objects, with space velocities typically several hundred km/s.^{11–14} Such high speeds are likely due a birth kick imparted at the time of the supernova, due to a combination of binary disruption (for sources initially enjoying a binary companion) and asymmetry in the supernova explosion itself. It is important to note that the known radio pulsar population is very incomplete and subject to strong observational selection biases; this is clear in Figure 1 wherein the locations of the radio pulsars on the Galactic disk are seen to be strongly clustered near Earth. These biases include those imposed by dispersion and scattering of radio waves by free electrons in the interstellar medium, by preferential surveying in the Galactic Plane, as well as by

^aCoincidentally, the year both of these authors were born.

^bThis quote appears in Ref. 7 but its origin is unspecified.

practical limits on time and frequency resolution in radio pulsar surveys. See for example Refs. 11, 15 for a discussion of selection effects in radio pulsar surveys.

Pulsars rotate rapidly, typically with rotation periods P of a few hundred ms. The presently known slowest radio pulsar has a period of ~ 8 s,¹⁶ while the fastest has period 1.4 ms or 716 Hz.¹⁷ All pulsars spin down steadily, a result of magnetic dipole braking, hence can be characterized by period P and its rate of change \dot{P} . The latter, though typically only tenths of microseconds per year, is eminently measurable for all known sources because of pulsars' famous rotational stability. Measurements of pulsar spin-down rate \dot{P} are extremely useful, as they enable helpful estimates of key physical properties.

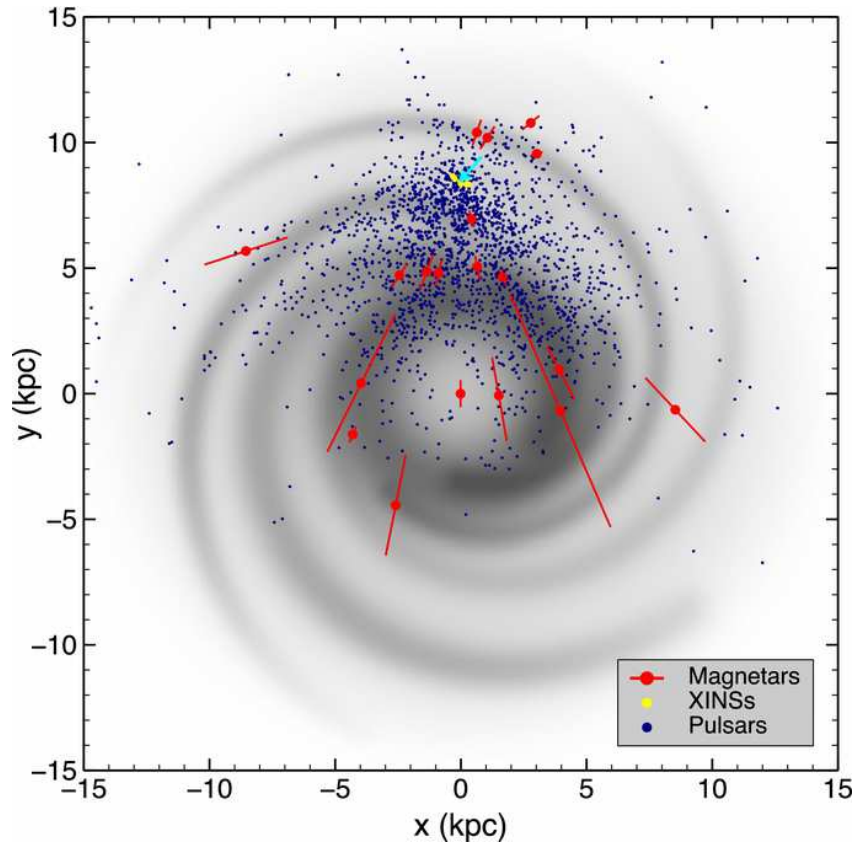


Fig. 1. Spatial distribution of radio pulsars (in blue), magnetars (in red; see §5), XDINS (aka XINS, in yellow; see §6), projected on the Galactic disk. The location of the Earth is indicated by a cyan arrow. The underlying grey scale roughly traces the free electron distribution. Figure taken from Olausen & Kaspi (2014).

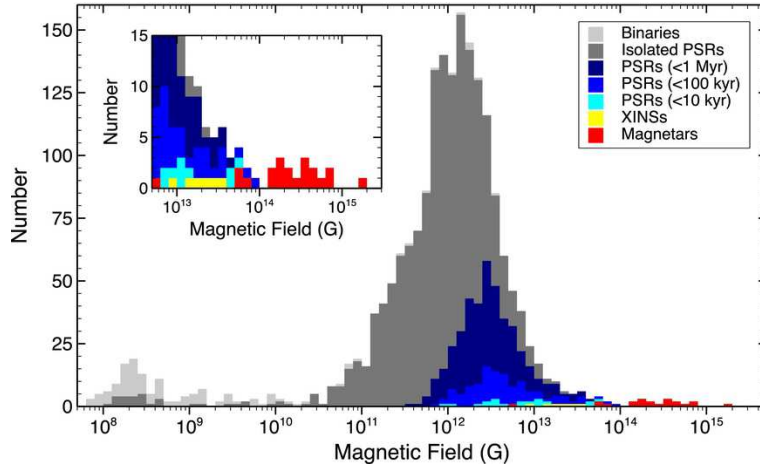
4 *Kaspi & Kramer*


Fig. 2. Distribution of spin-inferred magnetic fields (using Eq. 1) of radio pulsars (in various shades of blue and grey), XDINS (aka XINS, in yellow; see §6), and magnetars (in red; see §5). From Olausen & Kaspi (2014).

One such property is the surface dipolar magnetic field at the equator,

$$B = \left(\frac{3c^3 I}{8\pi^2 R^6} \right)^{1/2} \sqrt{P\dot{P}} = 3.2 \times 10^{19} \sqrt{P\dot{P}} \text{ G}, \quad (1)$$

where I is the stellar moment of inertia, typically estimated to be 10^{45} g cm^2 , and R is the neutron star radius, usually assumed to be 10 km (see Part II. for observational constraints.) This estimate assumes magnetic braking *in vacuo*, which was shown to be impossible early in the history of these objects¹⁸ since rotation-induced electric fields dominate over the gravitational force, even for these compact stars, such that charges must surely be ripped from the stellar surface and form a dense magnetospheric plasma. Nevertheless, modern relativistic magnetohydrodynamic simulations of pulsar magnetospheres have shown that the simple estimate offered by Eq. 1 is generally only a factor of 2–3 off.¹⁹ The observed distribution of radio pulsar magnetic fields is shown in Figure 2.

Measurement of P and \dot{P} also enable an estimate of the source’s age. The pulsar’s characteristic age τ_c is defined as

$$\tau_c = \frac{P}{(n-1)\dot{P}} \left[1 - \left(\frac{P}{P_0} \right)^{(n-1)} \right] \simeq \frac{P}{2\dot{P}}, \quad (2)$$

where n is referred to as the ‘braking index’ and is equal to 3 for simple magnetic dipole braking (see e.g. Ref. 7), though is observed to be less than 3 in the handful of sources for which a measurement of n has been possible.²⁰ P_0 is the spin period at birth and is generally assumed to be much smaller than the current spin period, although this is not always a valid assumption, particularly for young pulsars.²¹

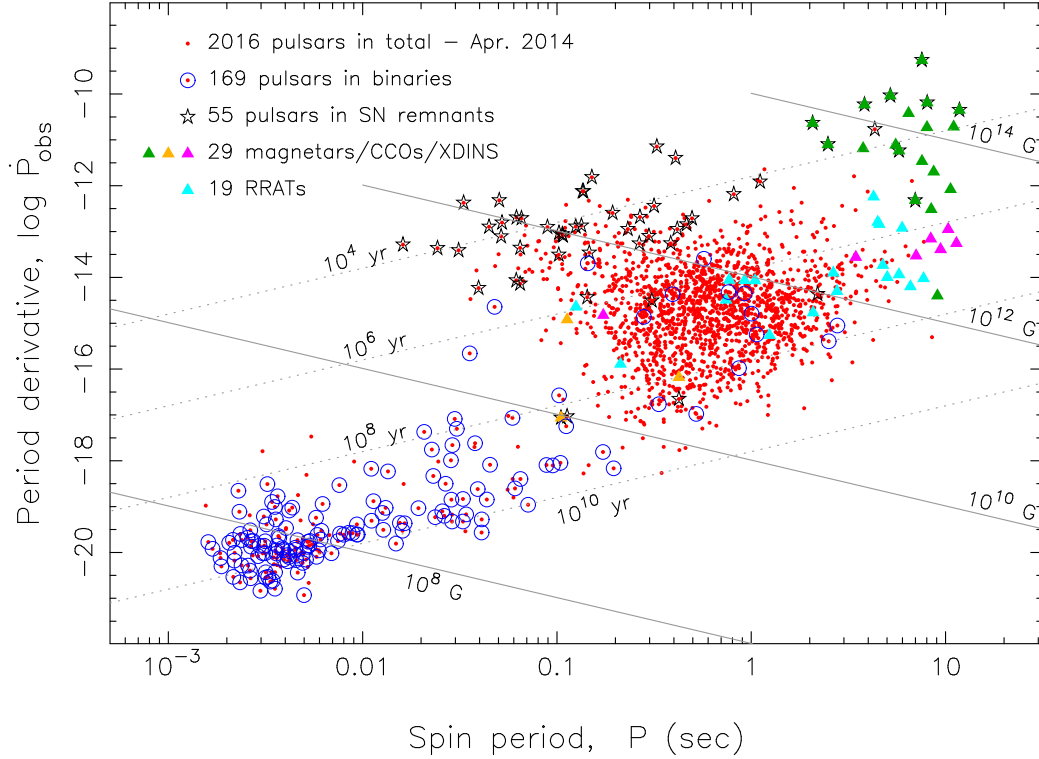


Fig. 3. P - \dot{P} diagram. Red dots indicate known radio pulsars as of April 2014. Blue circles represent binaries. Stars represent associated supernova remnants. Magnetars are represented by green triangles (see §5). The XDINS and CCOs (see §4,5) are pink and yellow triangles, respectively. RRATs (§9) are in cyan. Solid grey lines are of constant magnetic field (Eq. 1) and dotted lines are of constant characteristic age (Eq. 2). From Tauris et al. (2014).

Finally, a pulsar's spin-down luminosity L_{sd} (also known as \dot{E} , where $E \equiv \frac{1}{2}I\omega^2$ with $\omega \equiv 2\pi/P$ is the stellar rotational kinetic energy) can be estimated from P and \dot{P} and is given by

$$\dot{L}_{sd} = \frac{d}{dt} \left(\frac{1}{2}I\omega^2 \right) = I\omega\dot{\omega} = 4\pi^2 I \frac{\dot{P}}{P^3} = 4 \times 10^{31} \left(\frac{P_{-15} \dot{P}_{-15}}{P_1} \right) \text{ erg/s}, \quad (3)$$

where \dot{P}_{-15} is \dot{P} in units of 10^{-15} and P_1 is the period in units of seconds. L_{sd} represents the power available for conversion into electromagnetic radiation, an upper limit on the (non-thermal; see §2.1) radiation a pulsar can produce. For this reason, radio pulsars are also known as 'rotation-powered pulsars.'

A traditional way of summarizing the pulsar population is via the P - \dot{P} diagram (Fig. 3). Here the spin periods of pulsars are plotted on the x -axis and \dot{P} on the y -axis. The swarm of conventional radio pulsars clearly has its P peak near ~ 500 ms, with typical $B \simeq 10^{11}$ G and characteristic age $\tau_c \simeq 10^7$ yr. The youngest radio

pulsars have $\tau_c \simeq 1$ kyr and are generally found in supernova remnants; the latter dissipate typically after 10–100 kyr, explaining why older pulsars are generally not so housed in spite of all having been born in core-collapse supernovae. The $P = 33$ -ms Crab pulsar is arguably the most famous of the young pulsars, its birth having been recorded by Asian astrologers in 1054 A.D.²² However, it is in fact not the youngest known pulsar; this honour presently goes to the 884-yr old PSR J1846–0258 in the supernova remnant Kes 75.²³ Also clear in the P - \dot{P} diagram is the collection of binary pulsars, nearly all of which cluster in the lower left portion of the diagram, where the “millisecond pulsars” reside. This is no coincidence; although the rapid rotation of the young Crab-like pulsars is almost certainly a result of angular momentum conservation in the core collapse, that of the millisecond pulsars (MSPs) is intimately tied to their binarity. MSPs are believed to have been spun-up by an episode of mass accretion from their binary companion (see §3).

2.1. Pulsar Emission

Though rotation-powered pulsars are usually referred to as ‘radio pulsars,’ in reality these objects emit across the full electromagnetic spectrum. In fact, the radio emission (that in the ~ 100 MHz to ~ 100 GHz range), which must surely be of a non-thermal nature owing to the enormous brightness temperatures implied, usually represents a tiny fraction (typically $\sim 10^{-6}$) of L_{sd} , hence is energetically unimportant. The richness of radio observations and phenomenology has fuelled over the years significant theoretical effort into understanding its origin. However at present, there is no consensus and it remains an open question.^{24,25} In spite of the lack of an understanding of the physics of the radio emission, pulsar astronomers are generally content to accept its existence as coming from a ‘black box,’ and use it as an incredibly useful beacon of the dynamical behaviour of the star as described in Part II.

The second most commonly observed emission from rotation-powered pulsars is in the X-ray band. See Ref. 26 or 27 reviews. The origin of pulsar X-rays is far better understood than is the radio emission and we describe it briefly here as it is instructive, particularly when considering other classes of neutron stars (see §4). X-rays originate from one of two possible mechanisms, which can sometimes both be operating. One is thermal emission from the surface, due either to the star being initially hot following its formation in a core-collapse event (in which case the thermal luminosity need not be constrained by L_{sd}), or from surface reheating by return currents in the magnetosphere. The latter is particularly common in millisecond pulsars, but may well be present in all pulsars and indeed can be an important complicating factor in efforts to constrain neutron-star core composition via studies of cooling. As the thermal emission is thought to arise from the surface, it is typically characterized by quasi-sinusoidal pulsations, likely broadened by general relativistic light bending. The second source of X-rays is purely magnetospheric. This emission has a strongly non-thermal spectrum and is appears highly beamed, as observed via

very short duty-cycle pulsations. The non-thermal emission is ultimately powered by spin-down (as is the thermal return-current emission) so its luminosity must be limited by L_{sd} . Note that additional X-ray emission can be present in pulsars' immediate vicinity due to *pulsar wind nebulae* – sometimes spectacular synchrotron nebulae that result from pulsars' relativistic winds being confined by the ambient medium. See Ref. 28 for a review of these objects.

Space limitations preclude discussion of the third-most commonly observed emission band for rotation-powered pulsars – the gamma-ray regime. For a recent review of this interesting and highly relevant area of radio pulsar astrophysics, see Ref. 29.

3. Binary Radio Pulsars

As seen in Figure 3, pulsars with a binary companion generally, but not exclusively, inhabit the lower left of the $P-\dot{P}$ diagram, where spin periods are short and spin-down rates low. Indeed the vast majority of millisecond pulsars are in binary systems and have among the lowest magnetic field strengths of the pulsar population (see the small peak at the very low end in the B -field distribution in Fig. 2). These facts are not coincidental. According to the standard model,^{30–32} although the vast majority of radio pulsars originated from progenitors that were in binaries, most of these systems were disrupted by the supernova. Of the few that survived, subsequent evolution of the pulsar binary companion, under the right circumstances, resulted in Roche-lobe overflow and the transferring of matter and angular momentum onto the neutron star, in the process spinning it up. Such spun-up pulsars are often called “recycled” as they are effectively given a new life by their companion; without the latter they would have spun down slowly, alone, until ultimately the radio emission mechanism ceased as it eventually must. The mass transfer phase, observed as a bright accreting X-ray source powered by the release of gravitational energy as the transferred matter falls onto the neutron star,³² has a final result that depends strongly on the nature of the companion and its proximity to the neutron star. For low-mass companions, this mass transfer phase can last long enough to spin the pulsar up to millisecond periods. For higher-mass companions, only tens of millisecond periods can be achieved as these companions have shorter lifetimes. Simultaneous with the spin-up is an apparent quenching of the magnetic field, a process whose physics are poorly understood, but for which there is strong observational evidence. The above is a very broad-brush description of a very rich field of quantitative research that blends orbital dynamics with stellar evolution and neutron-star physics. One pictorial example of evolutionary scenarios that can lead to the formation of recycled pulsars is shown in Figure 4.³³

One outstanding mystery in the standard evolutionary model is the existence of isolated MSPs. These can be seen scattered in the lower left-hand part of Figure 3. Indeed, the first discovered MSP, PSR B1937+21, is isolated.³⁴ If binarity is key to recycling and spin-up, where are the isolated MSPs companions? One plausible answer may lie in the apparent companion ‘ablation’ that appears to be in progress

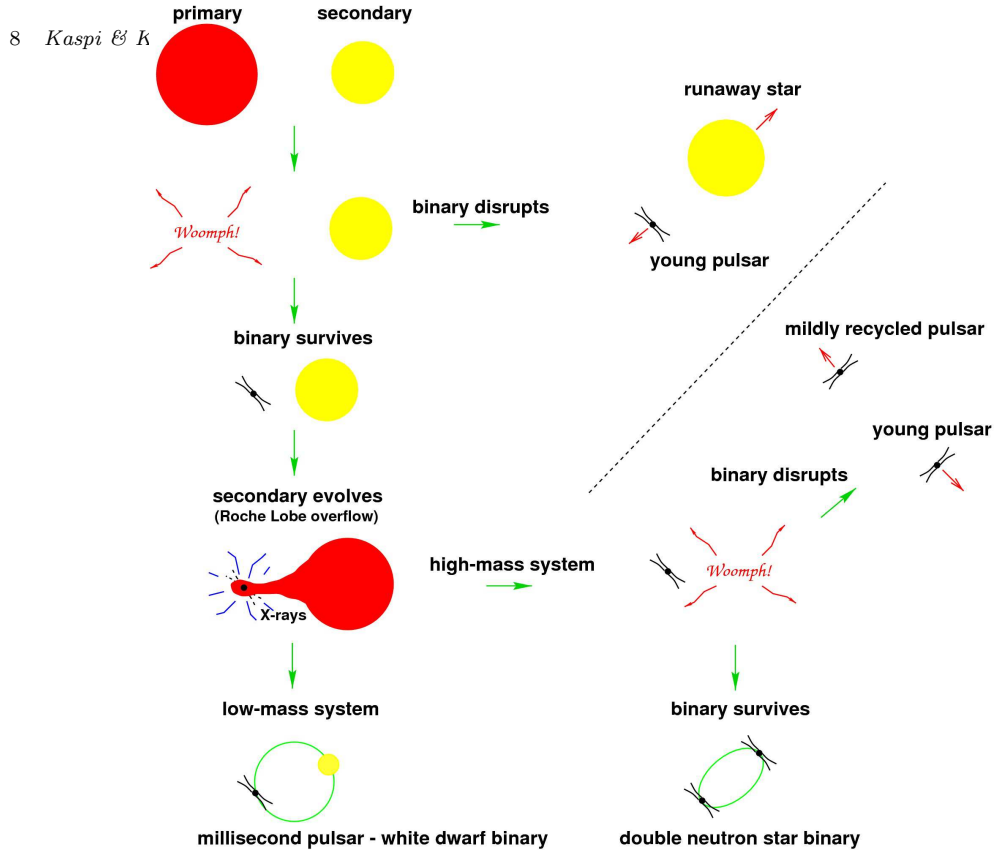


Fig. 4. Two neutron star binary evolution scenarios, one forming a millisecond pulsar – white dwarf binary, and the other a double neutron star binary. The primary deciding factor in the end state of the neutron star is the mass of its companion, with the white dwarf binary forming from a low-mass companion and the double neutron star from a high-mass companion. From Lorimer (2008).

in some close (orbital periods of a few hours) MSP binaries, notably those in which the radio pulsar is regularly eclipsed by material that extends well beyond the surface of the companion.^{35–37} The companion’s mass loss is believed to be fueled by the impingement of the intercepted relativistic pulsar particle wind which is ultimately powered by L_{sd} .

Another newly identified mystery is the discovery of eccentric MSP binaries. Key to the recycling process is rapid and efficient circularization of orbits and indeed some MSP binaries^{38,39} have eccentricities well under 10^{-6} . The discovery of an eccentricity 0.44 MSP in a 95-day orbit in the Galactic disk⁴⁰ thus was difficult to understand; one possibility is that it formed as part of a hierarchical triple system⁴¹ in which the inner companion was eventually ablated. The recent unambiguous detection of an MSP in a hierarchical triple system⁴² supports the existence of such systems, and suggests that binary evolution may be an incomplete picture of the paths to making MSPs.⁴³ Today there are 3 more MSP binary systems

having eccentricities $\gtrsim 0.1$ (Refs. 44, 8, 45) and though origins in triple systems are still on the table, other scenarios for their production, including accretion-induced collapse of a super-Chandrasekhar mass oxygen-neon-magnesium white dwarf in a close binary⁴⁶ and dynamical interaction with a circumbinary disk,⁴⁷ have been proposed.

Very recently, there has been a series of spectacular confirmations of key aspects of binary evolution theory. One is in the form of the discovery of a binary radio MSP, PSR J1023+0038, which had been observed to have an accretion disk in the previous decade.³⁷ Then there came the discovery of repeated swings between radio pulsations and bright accretion-powered X-ray pulsations in a different source.⁴⁸ Interestingly, the radio pulsations from PSR J1023+0038 have subsequently vanished⁴⁹ and a far brighter X-ray source has turned on,⁵⁰ suggesting some form of accretion, possibly in the propeller regime, is ongoing. Yet a third similar X-ray binary/radio MSP transitioning source has also recently been identified.⁵¹ This flurry of discoveries has brought us into a new era for making progress on the physics of accretion and accretion flows, the nature of the end of the recycling process and the formation of radio MSPs.

Finally, it is important to note the handful of radio pulsar binaries that sit among the regular population in the $P-\dot{P}$ diagram, i.e. young binaries in which the pulsar has not yet been recycled, and in which the companion is a massive main-sequence star. Only a few such objects are known⁵²⁻⁵⁴ likely owing to their short lifetimes. Unsurprisingly, these binaries are highly eccentric, resulting from a kick likely imparted at the time of the supernova explosion that formed the pulsar, but which (barely) did not unbind the orbit. These systems are interesting for a variety of reasons, including unusual dynamics present due to spin-induced quadrupole moments in the massive star, such as coupling between the stellar and orbital angular momenta.⁵⁵ This can cause precession in the system which can be used to detect misalignment between the stellar and orbital angular momenta, which provides strong evidence for a kick at the time of the neutron-star formation.⁵⁶⁻⁵⁸ Also, these systems provide a unique way to constrain the nature of massive star winds.^{59,60} One is also a γ -ray emitter,^{61,62} and serves as a possible ‘Rosetta Stone’ for a different class of γ -ray-emitting binaries in which the nature of the compact object is unknown.⁶³

4. Diversity in Neutron Stars

The last decade has shown us that the observational properties of neutron stars are remarkably diverse: Wheeler’s ‘handle and bell,’ invoked to describe emission from radio pulsars, now appears to be occasionally accompanied or sometimes substituted by a horn, a basket, a flashing light and/or a flag. It turns out, radio pulsars are just one observational manifestation of neutron stars. Today we have identified multiple other classes (or possibly sub-classes): magnetars (which have been sub-classified into ‘anomalous X-ray pulsars (AXPs)’ and ‘soft gamma repeaters (SGRs)’), X-

ray dim isolated neutron stars (XDINS), Central Compact Objects (CCOs), and Rotating Radio Transients (RRATs). In addition to an explosion of acronyms, we have an explosion of phenomenology. See Ref.⁶⁴ for a review. An important current challenge in neutron-star astrophysics is to establish an overarching physical theory of neutron stars and their birth properties that can explain this great diversity. Next we discuss each of these classes in turn.

5. Magnetars

Magnetars are without doubt the most dramatic of the neutron star population, with their hallmark observational trademark the emission of brief but intense – often greatly hyper-Eddington – X-ray and soft γ -ray bursts. This class of neutron stars was first noted in 1979 with the detection of repeated soft γ -ray bursts from two different sources by space-based detectors^{65,66} – hence the name ‘soft gamma repeater’ (SGR). Today there are 23 confirmed magnetars; the first magnetar catalog has been published⁶⁷ and is available online^c. See Ref. 68 for a very recent review. Three magnetars have shown particularly powerful “giant flares;”^{69,70} in the first 0.2 s of one such event, from SGR 1806–20, more energy was released than the Sun produces in a quarter of a million years⁶⁹ and in the first 0.125 s, the source outshone by a factor of 1000 all the stars in our Galaxy, with peak luminosity upwards of 2×10^{47} erg s⁻¹ and total energy released approximately 4×10^{46} erg.

Apart from their signature X-ray and soft γ -ray bursts, magnetars have the following basic properties. They are persistent X-ray pulsars, with periods for known objects in the range 2–12 s and are all spinning down, such that application of the standard magnetic braking formula (Eq. 1) yields field strengths typically in the range 10^{14} – 10^{15} G. In the past, two sub-classes have been referred to in the literature: the SGRs, and the ‘anomalous X-ray pulsars’ (AXPs) which, prior to 2002, had similar properties to the SGRs except did not seem to burst (but see below). Roughly 1/3 of all these sources are in supernova remnants, which clearly indicates youth; in very strong support of this is the tight confinement of Galactic magnetars (two are known in the Magellanic Clouds) to the Galactic Plane, with a scale height of just 20–30 pc.⁶⁷ This, along with some magnetar associations with massive star clusters,⁷¹ strongly suggests that magnetars are preferentially produced by very massive ($\gtrsim 30M_{\odot}$) stars that might otherwise have naively have been thought to produce black holes. Note that the magnetar spatial distribution in the Galaxy is subject to far fewer selection effects than is that of radio pulsars (see Fig. 1), because magnetars are typically found via their hard X-ray bursts (on which the interstellar medium has no effect) using all-sky monitors that have little to no preference for direction.

Importantly, and at the origin of their name, is that in many cases their X-ray luminosities and/or their burst energy outputs (and certainly the giant flare

^c<http://www.physics.mcgill.ca/~pulsar/magnetar/main.html>

energy outputs!) are orders of magnitude larger than what is available from their rotational kinetic energy loss, in stark contrast with conventional radio pulsars. Thus the main puzzle regarding these sources initially was their energy source. Accretion from a binary companion was ruled out early on given the absence of any evidence for binarity.⁷² Thompson and Duncan^{73–75} first developed the magnetar theory by arguing that an enormous internal magnetic field would be unstable to decay and could heat the stellar interior,⁷⁶ thereby stressing the crust from within, resulting in occasional sudden surface and magnetospheric magnetic restructuring that could explain the bursts. That same high field, they proposed, could explain magnetars' relatively long spin periods in spite of their great youth, as well as confine the energy seen in relatively long-lived tails of giant flares. The direct measurement of the expected spin-down rates⁷⁷ (and the implied spin-inferred magnetic fields mentioned above) came, crucially, after this key prediction. This provided the most powerful confirmation of the magnetar model; additional strong evidence came from the detection of magnetar-like bursts from the AXP source class^{78,79} which had previously been explicitly called out in Ref. 75 as being likely magnetars.

Although the magnetar model is broadly accepted by the astrophysical community, as for radio pulsars, a detailed understanding of their observational phenomena is still under development. Following the seminal theoretical work in Refs. 73, 74, 75, later studies have shown that magnetar magnetospheres likely suffer various degrees of 'twisting,' either on a global scale⁸⁰ or, more likely, in localised regions that have come to be called 'j-bundles'.⁸¹ The origin of sudden X-ray flux enhancements at the times of outburst may be in the development of these twists, with subsequent radiative relaxation coupled with field untwisting. On the other hand, interior heat depositions can also account for the observed flux relaxations post outburst, and, in this interpretation, can potentially yield information on crustal composition.^{82–84} Interesting open questions surround magnetar spectra, which are very soft below 10 keV, consisting of a thermal component that is rather hot ($kT \simeq 0.4$ keV) compared with those of radio pulsars (§2.1), and a non-thermal component that may arise from resonant Compton scattering of thermal photons by charges in magnetospheric currents. A sharp upturn in the spectra of magnetars above ~ 15 keV^{85,86} was unexpected but may be explainable of coronal outflow of e^\pm pairs which undergo resonant scattering with soft X-ray photons and lose their kinetic energy at high altitude.⁸⁷ Another magnetar mystery is that they are prolific glitchers,⁸⁸ in spite of apparently high interior temperatures that previously were invoked in the young and presumably hot Crab pulsar to explain its paucity of glitches.^{89,90} Also, some magnetar glitch properties are qualitatively different from those of radio pulsars, starting with their frequent (but not exclusive) association with bright X-ray outbursts.^{79,91,92}

5.1. *High- B Radio Pulsars and Magnetars*

One particularly interesting issue is how especially high- B radio pulsars relate to magnetars. Figure 2 shows histograms of the spin-inferred magnetic field strengths of radio pulsars (coloured by age) and magnetars. Although, generally speaking, magnetar field strengths are far higher than those of radio pulsars, there is a small overlap region in which there exist otherwise ordinary radio pulsars having magnetar-strength fields, and magnetars having rather low B fields.^{84,93} This is also easy to see in Figure 3. A partial answer to this comes from an event in 2006 in which the otherwise ordinary (though curiously radio quiet) rotation-powered pulsar PSR J1846–0258, albeit one with a moderately high B of 5×10^{13} G, suddenly underwent an apparent ‘magnetar metamorphosis,’ brightening by a factor of > 20 in the X-ray band and emitting several magnetar-like bursts.⁹⁴ This outburst lasted ~ 6 weeks, and then the pulsar returned to (nearly) its pre-outburst state. (See Ref. 95 for the post-outburst status.) This suggests that in high- B rotation-powered pulsars, there is the capacity for magnetar-type instabilities. Recent theoretical work on magnetothermal evolution in neutron stars supports this.^{96,97} Conversely, radio emission has now been detected from 4 magnetars,^{98–101} although it has interestingly different properties from that typical of radio pulsars. Notably it is often more variable, has an extremely flat radio spectrum, is essentially 100% linearly polarized and appears to be present only after outbursts, fading away slowly on time scales of months to years. One particularly interesting radio magnetar is SGR J1745–2900, found in the Galactic Centre, within $3''$ of Sgr A*.^{101–104} Though plausibly gravitationally bound to the black hole, its rotational instabilities (typical for magnetars) will likely preclude dynamical experiments.^{101,105} Nevertheless it is of considerable interest as its radio emission suffers far less interstellar scattering than expected given its location, suggesting future searches of the Galactic Centre region for more rotationally stable radio pulsars may bear fruit and allow sensitive dynamical experiments as described in Part II.

6. XDINS

The ‘X-ray Dim Isolated Neutron Stars’ (XDINS; also sometimes known more simply as Isolated Neutron Stars, INSs) are sub-optimally named neutron stars because (i) the term ‘dim’ is highly detector specific, and (ii) most radio pulsars are both neutron stars and ‘isolated.’ Nevertheless this name has stuck and refers to a small class that has the following defining properties: quasi-thermal X-ray emission with relatively low X-ray luminosity, great proximity, lack of radio counterpart, and relatively long periodicities ($P = 3–11$ s). For past reviews of XDINSs, see Refs. 27, 106, 107. XDINSs may represent an interestingly large fraction of all Galactic neutron stars;¹⁰⁸ we are presently only sensitive to the very nearest such objects (see Fig. 1). Timing observations of several objects have revealed that they are spinning down regularly, with inferred dipolar surface magnetic fields of typically a $\sim 1–3 \times 10^{13}$ G,^{107,109} and characteristic ages of $\sim 1–4$ Myr (see Fig. 3). Such fields

are somewhat higher than the typical radio pulsar field. This raises the interesting question of why the closest neutron stars should have preferentially higher B -fields. The favoured explanation for XDINS properties is that they are actually radio pulsars viewed well off from the radio beam. Their X-ray luminosities are thought to be from initial cooling and they are much less luminous than younger thermally cooling radio pulsars because of their much larger ages. However, their luminosities are too large for conventional cooling, which suggests an additional source of heating, such as magnetic field decay, which is consistent with their relatively high magnetic fields.

7. ‘Grand Unification’ of Radio Pulsars, Magnetars and XDINS: Magnetothermal Evolution

Recent theoretical work suggests that radio pulsars, magnetars and XDINS can be understood under a single physical umbrella as having such disparate properties simply because of their different birth magnetic fields and their present ages. Motivated largely by mild correlations between spin-inferred B and surface temperature in a wide range of neutron stars, including radio pulsars, XDINSs and magnetars¹¹⁰ (but see Ref. 111), a model of ‘magneto-thermal evolution’ in neutron stars has been developed in which thermal evolution and magnetic field decay are inseparable.^{97, 110, 112–114} Temperature affects crustal electrical resistivity, which in turn affects magnetic field evolution, while the decay of the field can produce heat that then affects the temperature evolution. In this model, neutron stars born with large magnetic fields ($> 5 \times 10^{13}$ G) show significant field decay, which keeps them hotter longer. The magnetars are the highest B sources in this picture, consistent with observationally inferred fields; the puzzling fact that XDINSs, in spite of their great proximity, appear to have high inferred B s relative to radio pulsars is explained as the highest B sources remain hottest, hence most easily detected, longest.

8. CCOs

A census of neutron-star classes should mention the so-called Central Compact Objects (CCO)^d. CCOs are a small, heterogeneous collection of X-ray emitting neutron-star-like objects at the centres of supernova remnants, but having puzzling properties which defy a clean classification. Properties common among CCOs are absence both of associated nebulae and of counterparts at other wavelengths. The poster-child CCO, discovered in the first-light observation of the *Chandra* observatory (Fig. 5), is the mysterious central object in the young oxygen-rich supernova remnant Cas A. Particularly puzzling is its lack of X-ray periodicity, lack of associated nebulosity, and unusual X-ray spectrum.^{115–118}

^dAgain, a rather poor name that has stuck: the Crab pulsar is certainly ‘central’ to its nebula and compact, nevertheless is *not* considered a CCO!

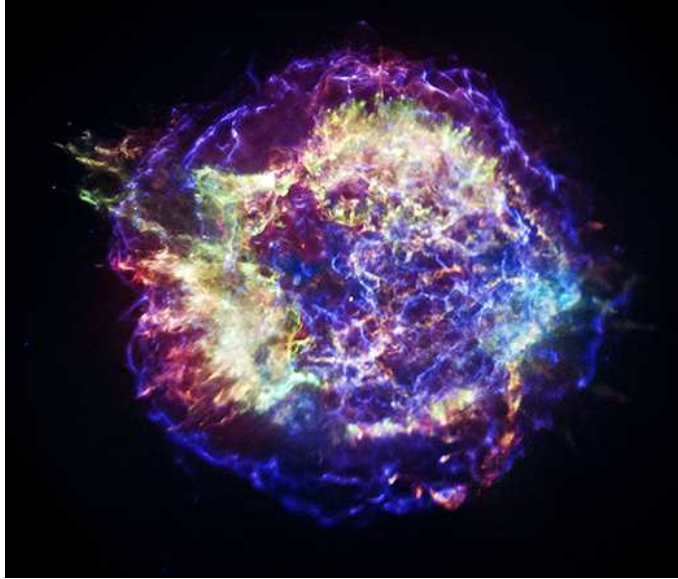


Fig. 5. X-ray image of the Cas A supernova remnant, obtained with the *Chandra* X-ray Observatory, showing the mysterious compact object at the centre. Image from <http://chandra.harvard.edu/photo/2013/casa/>.

Other objects that have been previously designated CCOs have been revealed to have low-level X-ray pulsations and surprisingly small spin-down rates. PSR J1852+0040 is at the centre of the SNR Kes 79.^{119,120} This undoubtedly young pulsar, observed only in X-rays, has $P = 105$ ms yet a magnetic field strength of only $B = 3.1 \times 10^{10}$ G. Its characteristic age, $\tau_c = 192$ Myr,¹²¹ is many orders of magnitude larger than the SNR age, and much older than would be expected for an object of its X-ray luminosity (which greatly exceeds the spin-down luminosity). Interestingly, the object sits in a sparsely populated region of the $P-\dot{P}$ diagram (Fig. 3), among mostly recycled binary pulsars. A similar case is the CCO in the SNR PKS 1209–52, 1E 1207.4–5209. This 0.4-s X-ray pulsar^{122,123} has a spin-down rate that implies $B = 9.8 \times 10^{10}$ G and age again orders of magnitude greater than the SNR age and inconsistent with a so large X-ray luminosity.¹²⁴ Yet another such low- B CCO is RX J0822–4300 in Puppis A,¹²⁵ with $P = 112$ ms and $B = 2.9 \times 10^{10}$ G.¹²⁴ Ref. 121 presents a synopsis of other sources classified as CCOs and argues that they are X-ray bright thanks to residual thermal cooling following formation, with the neutron star having been born spinning slowly. If so, the origin of the non-uniformity of the surface thermal emission is hard to understand. Even more puzzling however is the very high implied birthrate of these low- B neutron stars coupled with their extremely slow spin-downs: although none of these objects has yet shown radio emission, if one did, it should ‘live’ a very long time compared to higher- B radio pulsars, yet the region of the $P-\dot{P}$ diagram where CCOs should

evolve is greatly underpopulated in spite of an absence of selection effects against finding them (see also Ref. 64). This argues that for some reason, CCO-type objects must never become radio pulsars, which is puzzling, as there exist otherwise ordinary radio pulsars with CCO-like spin properties.

9. Rotating Radio Transients

No neutron-star census today is complete without a discussion of the so-called Rotating Radio Transients, or RRATs. RRATs are a curious class of Galactic radio sources¹²⁶ in which only occasional pulses are detectable, with conventional periodicity searches showing no obvious signal. Nevertheless, the observed pulses are inferred to occur at multiples of an underlying periodicity that is very radio-pulsar-like. Indeed, patient RRAT monitoring has shown that they also spin down at rates similar to radio pulsars. The number of known RRATs is now approximately 90^e, although just under 20 have spin-down rates measured. At first thought to be possibly a truly new class of neutron star, it now appears most reasonable that RRATs are just an extreme form of radio pulsar, which have long been recognized as exhibiting sometimes very strong modulation of their radio pulses.^{127, 128} Indeed several RRATs sit in unremarkable regions of the $P-\dot{P}$ diagram (Fig. 3). Interesting though is the mild evidence for longer-than-average periods and higher-than-typical B fields among the RRATs than in the general population. Regardless of whether RRATs are substantially physically different from radio pulsars, their discovery is important as it suggests a large population of neutron stars that was previously missed by radio surveys which looked only for periodicities. This may have important implications for the neutron-star birth rate and its consistency with the core-collapse supernova rate.^{108, 126}

10. Fast Radio Bursts: A New Mystery

Finally, a newly discovered class of radio sources – or rather, radio events – merits mention, even though they may or may not be related to neutron stars. Fast Radio Bursts (FRBs) are single, short (few ms), bright (several Jy), highly dispersed radio pulses whose dispersion measures suggest an origin far outside our Galaxy and indeed at cosmological distances.^f The first FRB reported¹³⁰ consisted of a single broadband radio burst lasting no longer than 5 ms from a direction well away from the Galactic Plane. The burst was extremely bright, with peak flux of 30 Jy, appearing for that moment as one of the brightest radio sources in the sky. The burst dispersion measure was a factor of 15 times the expected contribution from our Galaxy. Thornton et al. (2013) reported¹³¹ 4 more FRBs (see Fig. 6), demonstrating the existence of a new class of astrophysical events. Concerns that FRBs could be an

^eSee the online “RRatalog” at <http://astro.phys.wvu.edu/rratalog/rratalog.txt>

^fNote that FRBs are different in their properties from so-called “peryttons”, which turned out to be caused by local radio interference at the radio telescope site.¹²⁹

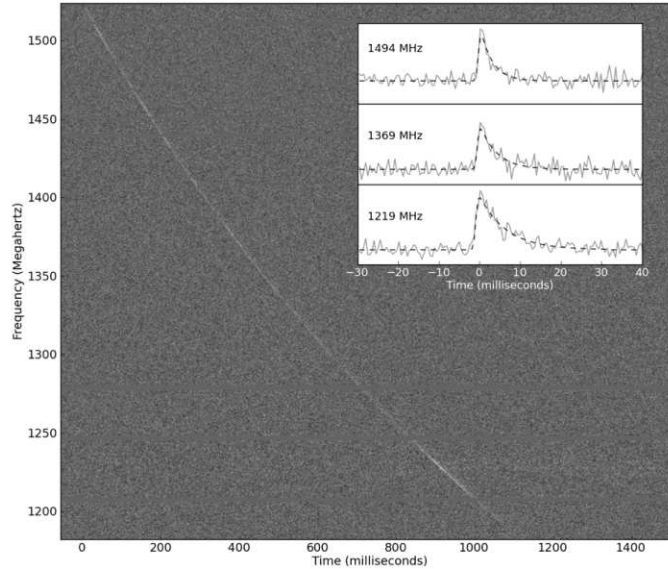


Fig. 6. One of the Thornton et al. (2013) FRBs. The telltale dispersion sweep of this single pulse is obvious across the radio band, and the burst profile at different radio frequencies is shown in the inset, where the radio-frequency dependence of the observed pulse broadening due to scattering is clear.

instrumental phenomenon (since the Lorimer FRB and those reported by Thornton were all found using the Parkes Observatory in Australia) have recently been laid to rest by the discovery¹³² of an FRB using the Arecibo telescope. Another FRB discovered in real-time¹³³ was found to be 14 – 20% circularly polarised on the leading edge. No linear polarisation was detected, although depolarisation due to Faraday rotation caused by passing through strong magnetic fields and/or high-density environments cannot be ruled out. The apparent avoidance of the Galactic Plane by FRBs is consistent with a cosmological origin¹³⁴ and an event rate of $\sim 10^4$ per sky per day,¹³¹ a surprisingly large number, albeit still based on small number statistics. Recent further data analysis and discoveries may suggest that this number may be a little smaller but still consistent with the previously estimated uncertainties (Champion, priv. comm.).

One may wonder, why it took six years since the first “Lorimer Burst” to discover further FRBs. This is due to the requirement to cover large areas of the sky with sufficient time and frequency resolution, combined with a need for sufficient computing power – areas, where recent modern surveys that are all based on digital hardware, are superior to their predecessors. Thus pulsar and RRAT hunters today are in unique positions to find FRBs, in particular with new instruments coming online that allow much larger fields-of-view.

The inferred large event rate and other FRB properties (DMs, widths, the pres-

ence of a scattering tail in some cases; see Fig. 6) demand an explanation. The locations on the sky of the known FRBs are determined only to several arcminutes, a region that typically contains many galaxies. Hence identification of a host galaxy – key for understanding the nature of the burster and its environment – has been impossible. Nevertheless, some models have been proposed; papers in the refereed literature have appeared faster than FRB detections! We discuss some of those models in Part II. with reference of their importance to fundamental physics.

FRBs are thus highly reminiscent of the now-famous ‘Gamma Ray Burst’ problem of the 1970s and 1980s – sudden, unpredictable burst events on the sky and difficult to localize – though with FRBs having the added difficulty of dispersion and the attendant great delay in detection presently due to computational demands. We cannot presently rule out that FRBs may represent a hitherto unrecognized type of astrophysical object, although as described below, neutron stars are also a plausible possibility.

Part II. - Neutron Stars as Laboratories for Fundamental Physics

As described above, the vast majority of neutron stars have been discovered in the radio regime in the form of radio pulsars. Putting aside astrophysical population and pulsar emission issues, radio observations of pulsars are important for totally independent reasons: they add to other techniques and methods employed to study fundamental physics with astronomical means. The latter include the study of a possible variation of fundamental constants across cosmic time using molecular spectroscopy of emission that originates from distant quasars. One can study the radio photons of the Cosmic Microwave Background (CMB) in great detail, as is being done as part of this conference. One can also use the coherent emission of water maser sources to obtain an accurate distance ladder to measure the local expansion of the Universe. Table 1 gives an overview of such experiments with references for further reading.

In the following, we will concentrate mostly on the study of gravitational physics where neutron star observations provide us with the best tests and constraints existing todate. Most of these tests are possible due to the rotational stability of neutron stars; the very large amount of stored rotational energy ($\sim 10^{44}$ W), in particular that of the fast rotating millisecond pulsars, makes them effective flywheels, delivering a radio “tick” per rotation with a precision that rivals the best atomic clocks on Earth. At the same time they are strongly self-gravitating bodies, enabling us to test not only the validity of general relativity, but also to probe effects predicted by alternative theories of gravity. They act as sources of gravitational wave (GW) emission, if they are in a compact orbit with a binary companion, but they may also act as detectors of low-frequency GWs in a so-called “pulsar timing array” (PTA) experiment, as we discuss next.

11. Tests of Theories of Gravity

The idea behind the usage of pulsars for testing general relativity (GR) and alternative theories of gravity is straightforward: if the pulsar is in orbit with a binary companion, we use the measured variation in the arrival times of the received signal to determine and trace the orbit of the pulsar about the common centre of mass as the former moves in the local curved space-time and in the presence of spin effects. In alternative theories, self-gravity effects are often expected, modifying also the orbital motion to be observed.

This “pulsar timing” experiment is simultaneously clean, conceptually simple and very precise. The latter is true since when measuring the exact arrival time of pulses at our telescope on Earth, we do a ranging experiment that is vastly superior in precision than a simple measurement of Doppler-shifts in the pulse period. This is possible since the pulsed nature of our signal links tightly and directly to the rotation of the neutron star, allowing us to count every single rotation. Furthermore, in this experiment we can consider the pulsar as a test mass that has a precision clock attached to it.

While, strictly speaking, binary pulsars move in the weak gravitational field of a companion, they do provide precision tests of the (quasi-stationary) strong-field regime. This becomes clear when considering that the majority of alternative theories predicts strong self-field effects which would clearly affect the pulsars’ orbital motion. Hence, tracing their fall in a gravitational potential, we can search for tiny deviations from GR, which can provide us with unique precision strong-field tests of gravity.

As a result, a wide range of relativistic effects can be observed, identified and studied. These are summarised in Table 2 in the form of limits on the parameters in the “Parameterised Post-Newtonian” (PPN) formalism (Ref. 135) and include concepts and principles deeply embedded in theoretical frameworks. If a specific alternative theory is developed sufficiently well, one can also use radio pulsars to test the consistency of this theory. Table 3 lists a number of theories where this has been possible. Sometimes, however, gravitational theories are put forward to explain certain observational phenomena without having studied the consequences of these theories in other areas of parameter space. In particular, alternative theories of gravity are sometimes proposed without having worked out their radiative properties, while in fact, tests for gravitational radiation provide a very powerful and sensitive probe for the consistency of the theory with observational data. In other words, every successful theory has to pass the binary pulsar experiments.

The various effects or concepts to be tested require sometimes rather different types of laboratory. For instance, in order to test the important radiative properties of a theory, we need compact systems, usually consisting of a pair of neutron stars. As we have seen, double neutron star systems (DNSs) are rare but they usually produce the largest observable relativistic effects in their orbital motion and, as we will see, produce the best tests of GR for strongly self-gravitating bodies. On the

other hand, to test the violation of the Strong Equivalence Principle, one would like to use a binary system that consists of different types of masses (i.e. with different gravitational self-energy), rather than a system made of very similar bodies, so that we can observe how the different masses fall in the gravitational potential of the companion and of the Milky Way. For this application, a pulsar-black hole system would be ideal. Unfortunately, despite past and ongoing efforts, we have not yet found a pulsar orbiting a stellar black hole companion or orbiting the supermassive black hole in the centre of our Galaxy.¹⁵⁵ Fortunately, we can use pulsar-white dwarf (PSR-WD) systems, as white dwarfs and neutron stars differ very significantly in their structure and, consequently, self-energies. Furthermore, some PSR-WD systems can also be found in relativistic orbits.^{9, 156}

12. The First Binary Pulsar – a Novel Gravity Laboratory

The first binary pulsar to ever be discovered happened to be a rare double neutron star system. It was discovered by Russel Hulse and Joe Taylor in 1974 (Ref. 157). The pulsar, B1913+16, has a period of 59ms and is in an eccentric ($e = 0.62$) orbit around an unseen companion with an orbital period of less than 8 hours. Soon after the discovery, Taylor and Hulse noticed that the pulsar does not follow the movement expected from a simple Keplerian description of the binary orbit, but that it shows the impact of relativistic effects. In order to describe the relativistic effects in a theory-independent fashion, one introduces so-called “Post-Keplerian” (PK) parameters that are included in a timing model to describe accurately the measured pulse times-of-arrival (see e.g. Ref. 158 for more details).

For the Hulse-Taylor pulsar, a relativistic advance of its periastron was soon measured analogous to what is seen in the solar system for Mercury, albeit with a much larger amplitude. The value measured today, $\dot{\omega} = 4.226598 \pm 0.000005$ deg/yr,¹⁵⁹ is much more precise than than was originally measured, but even early on the precision was sufficient to permit meaningful comparisons with GR’s prediction. The value depends on the Keplerian parameters and the masses of the pulsar and its companion:

$$\dot{\omega} = 3T_{\odot}^{2/3} \left(\frac{P_b}{2\pi} \right)^{-5/3} \frac{1}{1 - e^2} (m_p + m_c)^{2/3}. \quad (4)$$

Here, $T_{\odot} = GM_{\odot}/c^3 = 4.925490947\mu\text{s}$ is a constant, P_b the orbital period, e the eccentricity, and m_p and m_c the masses of the pulsar and its companion, respectively. See Ref. 158 for further details.

The Hulse-Taylor pulsar also shows the effects of gravitational redshift (including a contribution from a second-order Doppler effect) as the pulsar moves in its elliptical orbit at varying distances from the companion and with varying speeds. The result is a variation in the clock rate of with an amplitude of $\gamma = 4.2992 \pm 0.0008$ ms (Ref. 159). In GR, the observed value is related to the Keplerian parameters and

the masses as

$$\gamma = T_{\odot}^{2/3} \left(\frac{P_b}{2\pi} \right)^{1/3} e \frac{m_c(m_p + 2m_c)}{(m_p + m_c)^{4/3}}. \quad (5)$$

We can now combine these measurements. We have two equations with a measured left-hand side. On the right-hand side, we measured everything apart from two unknown masses. We solve for those and obtain, $m_p = 1.4398 \pm 0.0002 M_{\odot}$ and $m_c = 1.3886 \pm 0.0002 M_{\odot}$.¹⁵⁹ These masses are correct if GR is the right theory of gravity. If that is indeed the case, we can make use of the fact that (for point masses with negligible spin contributions), the PK parameters in each theory should only be functions of the *a priori* unknown masses of pulsar and companion, m_p and m_c , and the easily measurable Keplerian parameters (Ref. 160)[§]. With the two masses now being determined using GR, we can compare any observed value of a third PK parameter with the predicted value. A third such parameter is the observed decay of the orbit which can be explained fully by the emission of gravitational waves. And indeed, using the derived masses, along with the prediction of GR, i.e.

$$\dot{P}_b = -\frac{192\pi}{5} T_{\odot}^{5/3} \left(\frac{P_b}{2\pi} \right)^{-5/3} \frac{\left(1 + \frac{73}{24}e^2 + \frac{37}{96}e^4\right)}{(1 - e^2)^{7/2}} \frac{m_p m_c}{(m_p + m_c)^{1/3}}, \quad (6)$$

one finds an agreement with the observed value of $\dot{P}_b^{\text{obs}} = (2.423 \pm 0.001) \times 10^{-12}$ (Ref. 159) – however, only if a correction for a relative acceleration between the pulsar and the solar system barycentre is taken into account. As the pulsar is located about 7 kpc away from Earth, it experiences a different acceleration in the Galactic gravitational potential than does the solar system (see e.g. Ref. 158). The precision of our knowledge to correct for this effect eventually limits our ability to compare the GR prediction to the observed value. Nevertheless, the agreement of observations and prediction, today within a 0.2% (systematic) uncertainty,¹⁵⁹ represented the first evidence for the existence of gravitational waves. Today we know many more binary pulsars in which we can detect the effects of gravitational wave emission. In one particular case, the measurement uncertainties are not only more precise, but also the systematic uncertainties are much smaller, as the system is much more nearby. This system is the Double Pulsar.

13. The Double Pulsar

The Double Pulsar was discovered in 2003.^{161, 162} It not only shows larger relativistic effects and is much closer to Earth (about 1 kpc) than the Hulse-Taylor pulsar, allowing us to largely neglect the relative acceleration effects, but the defining unique property of the system is that it does not consist of one active pulsar and its *unseen* companion, but that it harbours two *active* radio pulsars.

One pulsar is mildly recycled with a period of 23 ms (named “A”), while the other pulsar is young with a period of 2.8 s (named “B”). Both orbit the common

[§]For alternative theories of gravity this statement may only be true for a given equation-of-state.

centre of mass in only 147-min with orbital velocities of 1 Million km per hour. Being also mildly eccentric ($e = 0.09$), the system is an ideal laboratory to study gravitational physics and fundamental physics in general. A detailed account of the exploitation for gravitational physics has been given, for instance, by Refs. 163, 164, 165. An update on those results is in preparation,¹⁴² with the largest improvement undoubtedly given by a large increase in precision when measuring the orbital decay. Not even ten years after the discovery of the system, the Double Pulsar provides the best test for the accuracy of the gravitational quadrupole emission prediction by GR far below the 0.1% level.

In order to perform this test, we first determine the mass ratio of pulsar A and B from their relative sizes of the orbit, i.e. $R = x_B/x_A = m_A/m_B = 1.0714 \pm 0.0011$.¹⁶³ Note that this value is theory-independent to the 1PN level.¹⁶⁶ The most precise PK parameter that can be measured is a large orbital precession, i.e. $\dot{\omega} = 16.8991 \pm 0.0001$ deg/yr. Using Eq. (4), this measured value and the mass ratio, we can determine the masses of the pulsars, assuming GR is correct, to be $m_A = (1.3381 \pm 0.0007) M_\odot$ and $m_B = (1.2489 \pm 0.0007) M_\odot$. The masses are shown, together with others determined by this and other methods, in Figure 7.

We can use these masses to compute the expected amplitude for the gravitational redshift, γ , if GR is correct. Comparing the result with the observed value of $\gamma = 383.9 \pm 0.6 \mu\text{s}$, we find that theory (GR) agrees with the observed value to a ratio of 1.000 ± 0.002 , as a first of five tests of GR in the Double Pulsar.

The Double Pulsar also has the interesting feature that the orbit is seen nearly exactly edge-on. This leads to a 30-s long eclipse of pulsar A due to the blocking magnetosphere of B that we discuss further below, but it also leads to a ‘‘Shapiro delay’’: whenever the pulse needs to propagate through curved space-time, it takes a little longer than travelling through flat space-time. At superior conjunction, when the signal of pulsar A passes the surface of B in only 20,000 km distance, the extra path length due to the curvature of space-time around B leads to an extra time delay of about 100 μs . The shape and amplitude of the corresponding Shapiro delay curve yield two PK parameters, s and r , known as *shape* and *range*, allowing two further tests of GR. s is measured to $s = \sin(i) = 0.99975 \pm 0.00009$ and is in agreement with the GR prediction of

$$s = T_\odot^{-1/3} \left(\frac{P_b}{2\pi} \right)^{-2/3} x \frac{(m_A + m_B)^{2/3}}{m_B}, \quad (7)$$

(where x is the projected size of the semi-major axis measured in lt-s) within a ratio of 1.0000 ± 0.0005 . It corresponds to an orbital inclination angle of 88.7 ± 0.2 deg, which is indeed very close to 90 deg as suggested by the eclipses. r can be measured with much less precision and yields an agreement with GR’s value given by

$$r = T_\odot m_B, \quad (8)$$

to within a factor of 0.98 ± 0.02 .

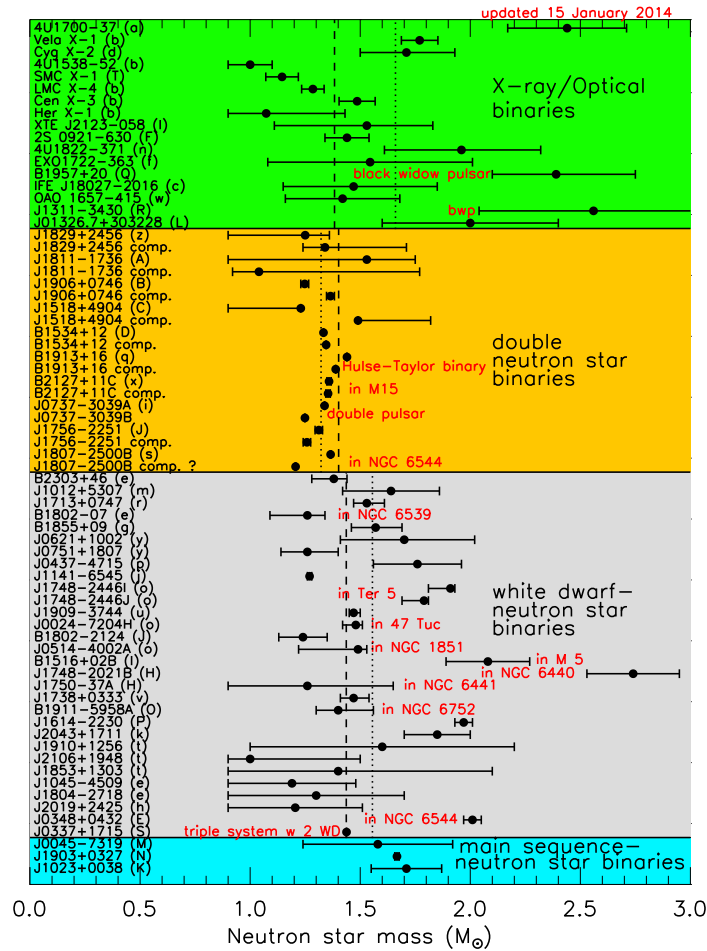


Fig. 7. Neutron star mass measurements compiled by J. Lattimer and available at www.stellarcollapse.org.

A fourth test is given by comparing an observed orbital decay of 107.79 ± 0.11 ns/day to the GR prediction. Unlike the Hulse-Taylor pulsar, extrinsic effects are negligible and the values agree with each other without correction to within a ratio of 1.000 ± 0.001 . This is already a better test for the existence of GW than possible with the Hulse-Taylor pulsar and will continue to improve with time. Indeed, at the

time of writing the agreement has already surpassed the 0.03% level.¹⁴²

14. Relativistic Spin-orbit Coupling

Apart from the Shapiro-delay, the impact of curved space-time is also immediately measurable by its effect on the orientation of the pulsar spin in a gyroscope experiment. This effect, known as geodetic precession or de Sitter precession represents the effect on a vector carried along with an orbiting body such that the vector points in a different direction from its starting point (relative to a distant observer) after a full orbit around the central object. Experimental verification has been achieved by precision tests in the solar system, e.g. by Lunar Laser Ranging (LLR) measurements, or recently by measurements with the Gravity Probe-B satellite mission (see Table 1). However, these tests are done in the weak field conditions of the solar system. Thus Pulsars currently provide the only access beyond weak-field, i.e. the quasi-stationary strong-field regime.

In binary systems one can interpret the observations, depending on the reference frame, as a mixture of different contributions to relativistic spin-orbit interaction. One contribution comes from the motion of the first body around the centre of mass of the system (de Sitter-Fokker precession), while the other comes from the dragging of the internal frame at the first body due to the translational motion of the companion.¹⁶⁷ Hence, even though we loosely talk about geodetic precession, the result of the spin-orbit coupling for binary pulsars is more general, and hence we will call it *relativistic spin-precession*. The consequence of relativistic spin-precession is a precession of the pulsar spin about the total angular momentum vector, changing the orientation of the pulsar relative to Earth.

Since the orbital angular momentum is much larger than the spin of the pulsar, the orbital angular momentum practically represents a fixed direction in space, defined by the orbital plane of the binary system. Therefore, if the spin vector of the pulsar is misaligned with the orbital spin, relativistic spin-precession leads to a change in viewing geometry, as the pulsar spin precesses about the total angular momentum vector. Consequently, as many of the observed pulsar properties are determined by the relative orientation of the pulsar axes towards the distant observer on Earth, we should expect a modulation in the measured pulse profile properties, namely its shape and polarisation characteristics.¹⁶⁸ The precession rate is another PK parameter and given in GR by (e.g. Ref. 158)

$$\Omega_p = T_\odot^{2/3} \left(\frac{2\pi}{P_b} \right)^{5/3} \frac{m_c(4m_p + 3m_c)}{2(m_p + m_c)^{4/3}} \frac{1}{1 - e^2}. \quad (9)$$

In order to see a measurable effect in any binary pulsar, *a)* the spin axis of the pulsar needs to be misaligned with the total angular momentum vector and *b)* the precession rate must be sufficiently large compared to the available observing time to detect a change in the emission properties. Considering these conditions, relativistic spin precession has now been detected in *all* systems where we can

realistically expect this.

As the most relativistic binary system known to date, we expect a large amount of spin precession in the Double Pulsar system. Despite careful studies, profile changes for A have not been detected, suggesting that A’s misalignment angle is less than a few degrees.¹⁶⁹ In contrast, changes in the light curve and pulse shape on secular timescales¹⁷⁰ reveal that this is not the case for B. In fact, B had been becoming progressively weaker and disappeared from our view in 2009.¹⁷¹ Making the assumption that this disappearance is solely caused by relativistic spin precession, it will only be out of sight temporarily until it reappears later. Modelling suggests that, depending on the beam shape, this will occur in about 2035 but an earlier time cannot be excluded.¹⁷¹ The geometry that is derived from this modelling is consistent with the results from complementary observations of spin precession, visible via a rather unexpected effect described in the following.

The change on the orientation of B also changes the observed eclipse pattern in the Double Pulsar, where we can see periodic bursts of emission of A during the dark eclipse phases, with the period being the full- or half-period of B. As this pattern is caused by the rotation of B’s blocking magnetospheric torus that allows light to pass B when the torus rotates to be seen from the side, the resulting pattern is determined by the three-dimensional orientation of the torus, which is centred on the precessing pulsar spin. Eclipse monitoring over the course of several years shows exactly the expected changes, allowing a determination of the precession rate to $\Omega_{p,B} = 4.77^{+0.66}_{-0.65}$ deg/yr. This value is fully consistent with the value expected in GR, providing a fifth test.¹⁴⁶ This measurement also allows us to test alternative theories of gravity and their prediction for relativistic spin-precession in strongly self-gravitating bodies for the first time (see Ref. 165 for details).

15. Alternative Theories of Gravity

Despite the successes of GR, a range of observational data has fuelled the continuous development of alternative theories of gravity. Such data include the apparent observation of “dark matter” or the cosmological results interpreted in the form of “inflation” and “dark energy,” as also discussed at this conference. Confronting alternative theories with data also in other areas of the parameter space (away from the CMB or Galactic scales), requires that these theories are developed sufficiently in order to make predictions. As mentioned, a particularly sensitive criterion is if the theory is able to make a statement about the existence and type of gravitational waves emitted by binary pulsars. Most theories cannot do this (yet), but a class of theories where this has been achieved is the class of tensor-scalar theories as discussed and demonstrated by Damour and Esposito-Farèse in a series of works (e.g. Ref. 172). For corresponding tests, the choice of a double neutron star system is not ideal, as the difference in scalar coupling, (that would be relevant, for instance, for the emission of gravitational *dipole* radiation) is small. The ideal laboratory would be a pulsar orbiting a black hole, as the black hole would have zero scalar

charge. The next best laboratory is a pulsar-white dwarf system. Indeed, such binary systems are able to provide constraints for alternative theories of gravity that are equally good or even better than solar system limits.¹³⁹

The previously best example for such a system was presented by Ref. 139, who reported the results of a 10-year timing campaign on PSR J1738+0333, a 5.85-ms pulsar in a practically circular 8.5-h orbit with a low-mass white dwarf companion. A large number of precision pulse time-of-arrival measurements allowed the determination of the intrinsic orbital decay due to gravitational wave emission. The agreement of the observed value with the prediction of GR introduces a tight upper limit on dipolar gravitational wave emission, which can be used to derive the most stringent constraints ever on general scalar-tensor theories of gravity. The new bounds are more stringent than the best current Solar system limits over most of the parameter space, and constrain the matter-scalar coupling constant α_0^2 to be below the 10^{-5} level. For the special case of the Jordan-Fierz-Brans-Dicke theory, the authors obtain a one-sigma bound of $\alpha_0^2 < 2 \times 10^{-5}$, which is within a factor of two of the Solar-System Cassini limit.^{139, 173} Moreover, their limit on dipolar gravitational wave emission can also be used to constrain a wide class of theories of gravity which are based on a generalisation of Bekenstein’s Tensor-Vector-Scalar (TeVeS) gravity, a relativistic formulation of Modified Newtonian Dynamics (MOND).¹⁷⁴ They find that in order to be consistent with the results for PSR J1738+0333, these TeVeS-like theories have to be fine-tuned significantly (see Table 3). We expect the latest Double Pulsar results to close a final gap of parameter space left open by the PSR-WD systems.^{139, 142}

A recently studied pulsar-white dwarf system^{9, 143} turned out to be a very exciting laboratory for various aspects of fundamental physics: PSR J0348+0432 harbours a white dwarf whose composition and orbital motion can be precisely derived from optical observations. The results allow us to measure the mass of the neutron star, showing that it has a record-breaking value of $2.01 \pm 0.04 M_\odot$!¹⁴³ This is not only the most massive neutron star known (at least with reliable precision), providing important constraints on the “equation-of-state” (see below) but the 39-ms pulsar and the white dwarf orbit each other in only 2.46 hours, i.e. the orbit is only 15 seconds longer than that of the Double Pulsar. Even though the orbital motion is nearly circular, the effect of gravitational wave damping is clearly measured. Hence, the high pulsar mass and the compact orbit make this system a sensitive laboratory of a previously untested strong-field gravity regime. Thus far, the observed orbital decay agrees with GR, supporting its validity even for the extreme conditions present in the system.¹⁴³ The precision of the observed agreement is already sufficient to add significant confidence to the usage of GR templates in the data analysis for gravitational wave (GW) detectors.

16. Pulsars as Gravitational Wave Detectors

The observed orbital decay in binary pulsars detected via precision timing experiments so far offers the best evidence for the existence of gravitational wave (GW) emission. Intensive efforts are therefore ongoing world-wide to make a direct detection of gravitational waves that pass over the Earth. Ground-based detectors like GEO600, VIRGO or LIGO use massive mirrors, the relative separations of which are measured by a laser interferometer set-up, while the envisioned space-based LISA detector uses formation flying of three test-masses that are housed in satellites. For a summary of these efforts, see, e.g. Ref. 135.

The change of the space-time metric around the Earth also influences the arrival times of pulsar signals measured at the telescope. Therefore, pulsars do not only act as sources of GWs, but they may eventually also lead to their direct detection. Fundamentally, the GW frequency range that pulsar timing is sensitive to, is bound by the cadence of the timing observations on the high frequency side, and by the length of the data set on low-frequency part. Hence, typically GWs with periods of the order of one year or more could be detected. Since GWs are expected to produce a characteristic quadrupole signature on the sky, the timing residuals from various pulsars should be correlated correspondingly,¹⁷⁵ so that the comparative timing of several pulsars can be used to make a detection. The sensitivity of such a ‘‘Pulsar Timing Array’’ (PTA) increases with the number of pulsars and should be able to detect gravitational waves in the nHz regime, hence below the frequencies to which LIGO (\sim kHz and higher) and LISA (\sim mHz) are sensitive. Sources in the nHz range (see, e.g., Ref. 176) include astrophysical objects (i.e. super-massive black hole binaries resulting from galaxy mergers in the early Universe), cosmological sources (e.g. the vibration of cosmic strings), and transient phenomena (e.g. phase transitions).

A number of PTA experiments are ongoing, namely in Australia, Europe and North America (see Ref. 177 for a summary). The currently derived upper limits on a stochastic GW background (e.g. Refs. 178) are very close to the theoretical expectation for a signal that originates from binary supermassive black holes expected from the hierarchical galaxy evolution model.^{179,180}

But the science that can eventually be done with the PTAs goes far beyond simple GW detection – a whole realm of astronomy and fundamental physics studies will become possible. The dominant signal in the nHz regime is expected to be a stochastic background due to merging supermassive black holes and many constraints can be placed on this source population, including their frequency in cosmic history, the relation between the black holes and their hosts, and their coupling with the stellar and gaseous environments.^{181,182} Detection of gas disks surrounding merging supermassive black holes and related eccentricities in such systems is possible;^{183,184} PTAs should be able to constrain the solution to the famous ‘last parsec problem’.¹⁸⁵ In addition to detecting a *background* of GW emission, PTAs can detect *single* GW sources. We can, for instance, expect to detect anisotropies

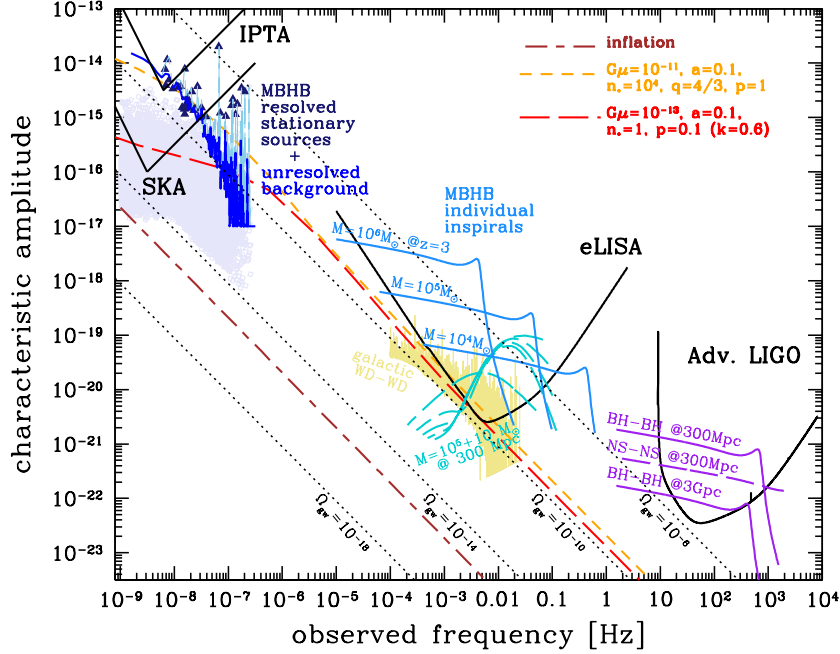


Fig. 8. The gravitational wave spectrum with expected sources. Shown is the characteristic amplitude vs. frequency as presented by Janssen et al. (2015): In the nHz regime, individually resolvable systems and the level of the unresolved background are indicated. Nominal sensitivity levels for the IPTA and SKA are also shown. In the mHz frequency range, the eLISA sensitivity curve is shown together with typical circular SMBHB inspirals at $z=3$ (pale blue), the overall signal from Galactic WD-WD binaries (yellow) and an example of extreme mass ratio inspiral (aquamarine). In the kHz range an advanced LIGO curve is shown together with selected compact object inspirals (purple). The brown, red and orange lines running through the whole frequency range are expected cosmological backgrounds from standard inflation and selected string models, as labeled in figure.

in a GW background, due to the signals of single nearby supermassive black hole binaries.^{186,187} Considering the case when the orbit is effectively not evolving over the observing span, we can show that, by using information provided by the “pulsar term” (i.e. the retarded effect of the GW acting on the pulsar’s surrounding space-time), we may be able to achieve interesting (~ 1 arcmin) source localisation.¹⁸⁶ Even astrophysical measurements of more local relevance can be done with PTAs; for example an independent determination of the masses of the Jovian planetary system has already been made (Ref. 188) and additional future, improved measurements for Jupiter and other planets should be possible. On the fundamental physics side, departures from GR during supermassive black hole mergers should be measurable via different angular dependences of pulsar timing residuals on the sky such as for example from gravitational wave polarization properties that differ from those predicted by GR.^{189–191} It may even be possible to constrain the mass of the graviton from the angular correlation of pulsar timing residuals.¹⁹² If the on-

going PTA experiments do not detect GWs in the next few years, a first detection is virtually guaranteed with the more sensitive Phase I of the Square Kilometer Array.¹⁷⁶ With even further increased sensitivity of SKA Phase II, it should also be possible to study the fundamental properties of gravitational waves.

17. Black Holes or the Centre of the Galaxy as a Gravity Lab

What makes a binary pulsar with a black-hole companion so interesting is that it has the potential of providing a superb new probe of relativistic gravity. As pointed out by Ref. 193, the discriminating power of this probe might supersede all its present and foreseeable competitors. The reason lies in the fact that such a system would clearly expose the self-field effects of the body orbiting the black hole, hence making it an excellent probe for alternative theories of gravity.

But also for testing the black hole properties predicted by GR, a pulsar-BH system will be superb laboratory. Ref. 194 was the first to provide a detailed recipe for how to exploit a pulsar-black hole system. They showed that the measurement of spin-orbit coupling in a pulsar-BH binary in principle allows us to determine the spin and the quadrupole moment of the black hole. This could test the “cosmic censorship conjecture” and the “no-hair theorem”. While Ref. 194 showed that with current telescopes such an experiment would be almost impossible to perform (with the possible exception of pulsars about the Galactic centre black hole), Ref. 195 pointed out that the SKA sensitivity should be sufficient. Indeed, this experiment benefits from the SKA sensitivity in multiple ways. It provides the required timing precision while also enabling deep searches, enabling a Galactic Census which should eventually deliver the desired sample of pulsars with a BH companion. As shown recently,¹⁹⁶ with the SKA or the *Five-hundred-meter Aperture Spherical radio Telescope* (FAST) project¹⁹⁷ one could test the cosmic censorship conjecture by measuring the spin of a stellar black hole, though it is still unlikely to find a system that can enable the measurement of the quadrupole moment.

As the effects become easier to measure with more massive black holes, the best laboratory would be a pulsar orbiting the central black hole in the Milky Way, Sgr A*.^{194, 195, 198} Indeed, Ref. 155 continued the work of Ref. 194 and studied this possibility in detail. They showed that it should be “fairly easy” to measure the spin of the GC black hole with a precision of $10^{-4} - 10^{-3}$. Even for a pulsar with a timing precision of only 100 μ s, characteristic periodic residuals would enable tests of the no-hair theorem with with a precision of one percent or better!

17.1. *Pulsars in the Galactic Centre*

Unfortunately, searches for pulsars near Sgr A* have been unsuccessful for the last 30 years - until April 2013. As described in Section 5.1, a radio signal of the 3.7-s magnetar J1745–2900 was detected.^{101, 104} The source has the highest dispersion measure of any known pulsar, is highly polarised and has a rotation measure that is larger than that of any other source in the Galaxy, apart from Sgr A*. This, and the

fact that VLBI images of the magnetar show scattering identical to that in the radio image of Sgr A* itself,¹⁹⁹ support the idea that the source is indeed only ~ 0.1 pc away from the central black hole. Initially, measurements of the scatter-broadening of the single radio pulses²⁰⁰ suggested that scattering due to the inner interstellar medium is too small to explain the lack of pulsar detection in previous survey. Recent preliminary results, enabled by the the puzzling fact that the radio emission remains unabated in spite of significant source fading in the X-ray band,²⁰¹ show an increase of scattering, indicating that the conditions are instead highly changeable (Spitler et al. in prep.). The fact that a rare object like a radio-emitting magnetar is found in such proximity to Sgr A* suggests that estimates like that of Ref. 202, predicting as many as 1000 pulsars in the inner central parsec, may indeed be true. Further searches are ongoing but may require observations at very high (i.e. ALMA) frequencies, i.e. > 40 GHz to beat the extreme scattering, which decreases as $\sim \nu^{-4}$.

17.2. The Event Horizon Telescope & BlackHoleCam

Telescopes operating at high radio frequencies may not only allow us to find a pulsar in the Galactic Centre, but combined with other radio telescopes, they can also form an interferometer to take an image of Sgr A* that can resolve the “shadow” of the supermassive black hole in the centre of our Milky Way. With a mass of about $4.3 \times 10^6 M_{\odot}$ ^{203,204} it is not very large in size compared to those in the centres of other galaxies, but it is the closest. The image to be taken by the so-called “Event Horizon Telescope” and “BlackHoleCam” experiments (see e.g. Ref. 205 for a recent review) will depend on the magnitude and direction of Sgr A*’s spin, i.e. information available by the discovery of pulsar around the central black hole, as described above. Combined measurements probe simultaneously the near- and far-field of Sgr A*, promising a unique probe of gravity.

18. Physics at Extreme Densities

The density of pulsars and neutron stars is so large that their matter cannot be reproduced in terrestrial observatories. Therefore, in order to understand how matter behaves under very extreme condition, observations of pulsars provide unique insight. On one hand, mass measurements constrain the Equation-of-State (EOS) at the highest densities, which also affects the maximum possible spin frequency of pulsars¹⁷ and sets bounds to the highest possible density of cold matter (see contribution by J. Lattimer). Because, a given EOS describes a specific mass-radius relationship (see, e.g., Ref. 206), measurements of the radii of neutron stars also set constrains on the EOS near nuclear saturation density and yield information about the density dependence of the nuclear symmetry energy.^{149,207} In practice, mass measurements are easier to achieve than radius measurements – or the discovery of sub-millisecond pulsars with significantly faster spin-periods than currently known.¹⁷ Specifically, while there are about 40 neutron star masses known with

varying accuracy (see Figure 7), there are no precise simultaneous measurements of mass and radius for any neutron star.

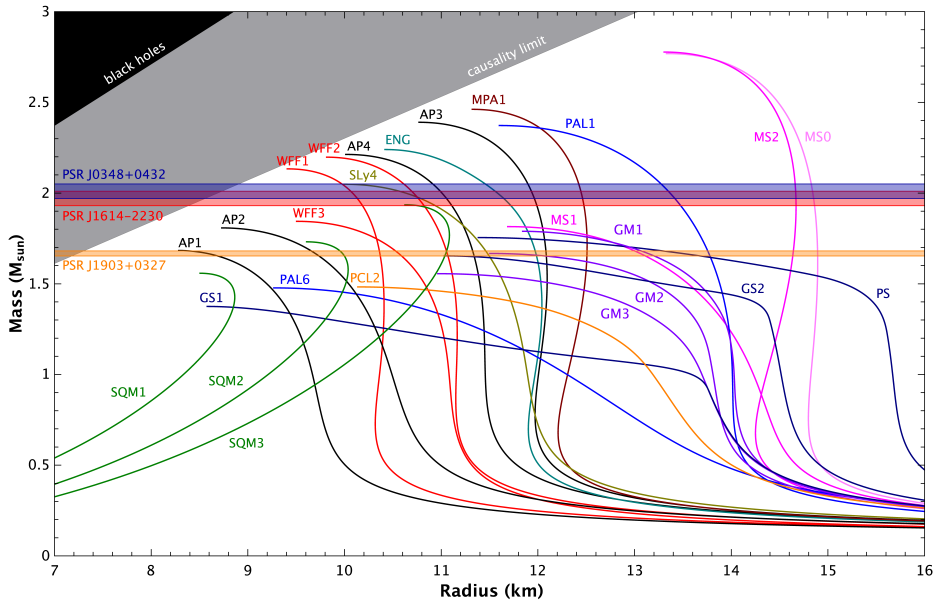


Fig. 9. Constraints on the equation-of-state provided by mass measurements of the most massive neutron stars. Figure provided by N. Wex. For details see e.g. Demorest et al. (2010).

For now, some of the best constraints for the EOS come simply from the maximum observed neutron star mass. Unlike in Newtonian physics, in GR a maximum mass exists as for any causal EOS as the isothermal speed of sound must never exceed the speed of light. Currently, the largest masses are measured for PSR J1614+2230 with $M = 1.94 \pm 0.04 M_{\odot}$ ¹⁴⁸ and PSR J0348+0432 with $M = 2.01 \pm 0.04 M_{\odot}$.¹⁴³ These independent measurements confirm the existence of high-mass neutron stars, ruling out a number of soft EOS already (see Figure 9). However, as explained, for instance, in Ref. 207, this lower limit on the maximum mass also provides constraints on the EOS at lower densities and on the radii of intermediate mass neutron stars. In general, however, most radii estimates come from estimates inferred from photospheric radius expansion bursts and thermal X-ray emission from neutron star surfaces. A Bayesian analysis of the existing data suggests a radius range of 11.3–12.1 km for a $1.4 M_{\odot}$ neutron star.^{149,207}

In terms of information about fundamental properties of super-dense matter, the *maximum* mass of neutron stars is clearly important. Small mass measurements, in particular those below $1.20 M_{\odot}$, are nevertheless extremely interesting from a neutron-star formation point-of-view as they would call into question the gravitational-collapse formation scenario.²⁰⁷ One way to form such low-mass neu-

tron stars is through electron-capture supernovae. Here, a white dwarf with an oxygen-neon-magnesium (O-Ne-Mg) core collapses to a low-mass neutron star due to electron captures on Ne and/or Mg, as was proposed for the formation of the light companion in the Double Pulsar system, PSR J0737–3039B.²⁰⁸ It was suggested that electron capture could be triggered in particular in close binaries. Assuming minimal mass loss, the final mass should be determined by the mass of the progenitor star minus the binding energy. As for any given EOS one can calculate the relation between the gravitational mass and the baryonic mass, one can in principle use the observed mass and the small mass range expected for an e-capture progenitor ($M_0 \sim 1.366 - 1.375M_\odot$) to constrain the EOS.²⁰⁸ However, alternative ways of producing such light neutron stars, e.g. via ultra-stripped Type Ic Supernovae from close binary evolution,²⁰⁹ have been proposed also.

The Double Pulsar may also allow us to actually measure the moment-of-inertia of a neutron star. As this combines the mass and the radius of a neutron star in one observable directly, such a measurement would be very significant in determining the correct EOS.^{162,210} Indeed, a measurement of the moment-of-inertia of pulsar A in the Double Pulsar, even with moderate accuracy ($\sim 10\%$), would provide important constraints.^{210–212} Recent timing results revealing 2PN-effects at the required level give hope that this goal can be reached eventually.¹⁴² See Ref. 165 for a detailed review on the prospects for making such measurement.

19. Fast Radio Bursts, Revisited

In Part I we introduced a new type of transient radio sources now known as Fast Radio Bursts (FRBs). In the context of fundamental physics, we are interested in exploring their nature on the one hand, and their usage as probes on the other. As their origin is still unclear, we will only attempt to give an overview of the existing, fast growing literature. We start with looking at the origin of FRBs.

All FRBs detected follow a perfect ν^{-2} -dispersion law, as it is expected from signal propagation in a cold ionized medium. In the discussion, whether the signals are Galactic or extra-galactic, Ref. 213 proposed FRBs may actually be Galactic flare stars wherein the large dispersion measure is due to dense plasma in low-mass star atmospheres, rather than a demonstration of a large distance traversed. However Refs. 214, 215, 216 reject this Galactic model using radiation transfer arguments; e.g. such high plasma densities should produce enormous intrinsic absorption that should render them undetectable, or produce free-free emission that is not seen, or result in a break-down of the cold plasma dispersion law, which contradicts observations. Moreover, a number of FRBs also show signs for interstellar scattering. Where it has been possible to measure (e.g. Ref. 131; see Fig. 6), the frequency dependence of the scattering time follows a ν^{-4} -law, as expected for propagation in interstellar and intergalactic space. With the dispersion measure (typically vastly) exceeding the contribution expected from the Milky Way, an extra-galactic origin is the most likely explanation, with distances corresponding to redshifts of the order

of $z \sim 1$ as inferred from an estimate of the intergalactic free electron content.¹³¹

From the combination of temporal brevity and great luminosity (inferred from their large distances), we then immediately infer that the sources must embody a physically extreme environment, likely involving very high gravitational or magnetic fields. Possibilities being discussed include interacting magnetospheres of coalescing neutron stars, coalescing white dwarfs, evaporating black holes, supernovae, and super-giant pulses (see Refs. 131, 217 and references therein). More exotic models propose signals from (bare) strange stars,²¹⁸ white holes,²¹⁹ or super-conducting cosmic strings.²²⁰ FRB emission must almost certainly be from a coherent process as the implied brightness temperature for a thermal process is impossibly large given the small size implied by the short durations; considering less exotic models, one would there expect that FRBs originate from some sort of compact object – white dwarf, neutron star or black hole. One possibility that appears particularly appealing based on expected event rates is giant magnetar flares.^{216, 221}

Whatever FRBs turn out to be, as extragalactic transient signals, they promise to be very useful cosmological probes. For example, their dispersion measure enables us to account for the ionized baryons between us and the FRB sources and to measure the curvature of spacetime through which the radiation propagates. A number of recent publications discuss these possibilities, many of which are very well summarized in Ref. 222. Generally, they fall in three categories, i.e. FRBs as locators of the missing baryons in the low ($z \leq 2$) redshift universe, high-redshift cosmic rulers which have the potential to determine the equation-of-state parameter w over a large fraction of cosmic history, or potential probes of primordial (intergalactic) magnetic fields and turbulence. See Ref. 222 for more details.

Summary & Conclusions

As we hope we have shown in this review, the field of neutron star research, and in particular radio pulsars, is extremely active, and addresses a very broad diversity of physical and astrophysical questions. These range from the structure and physics of dense supra-nuclear matter, to the fate and evolution of massive stars, to the nature of gravity and the origins of the Universe and the structure therein. We challenge our Solvay conference colleagues to identify an astrophysical area more replete with results and impact! The future for this domain of astrophysical research appears to be growing only brighter, buoyed in particular by the development and proliferation of multiple major new radio telescopes, including LOFAR, MWA, ALMA, Meerkat, ASKAP, CHIME, FAST, and in the next decade, SKA. Moreover, this science goes hand-in-hand with the blossoming field of astrophysical transients, whether considering magnetar bursts as possible FRB progenitors, or considering NS-NS mergers as aLIGO/VIRGO sources. We look forward to either participating in or hearing the results reported at the next Solvay astrophysics meeting (which will hopefully take place in fewer years than have passed since the last!) by which time we predict there will have been major discoveries in gravitational wave physics, in gravity in

general, and in neutron-star astrophysics.

References

1. J. Chadwick, *Nature* **192** (1932) 312.
2. W. Baade and F. Zwicky, *Phys. Rev.* **45** (1934) 138.
3. A. Hewish, S. J. Bell, J. D. H. Pilkington, P. F. Scott and R. A. Collins, *Nature* **217** (1968) 709.
4. I. S. Shklovsky, *ApJL* **148** (1967) L1.
5. T. Gold, *Nature* **221** (1969) 25.
6. F. Pacini, *Nature* **219** (1968) 145.
7. R. N. Manchester and J. H. Taylor, *Pulsars* (Freeman, San Francisco, 1977).
8. E. D. Barr, D. J. Champion, M. Kramer, R. P. Eatough, P. C. C. Freire, R. Karuppusamy, K. J. Lee, J. P. W. Verbiest, C. G. Bassa, A. G. Lyne, B. Stappers, D. R. Lorimer and B. Klein, *MNRAS* **435** (2013) 2234.
9. R. S. Lynch, J. Boyles, S. M. Ransom, I. H. Stairs, D. R. Lorimer, M. A. McLaughlin, J. W. T. Hessels, V. M. Kaspi, V. I. Kondratiev, A. M. Archibald, A. Berndsen, R. F. Cardoso, A. Cherry, C. R. Epstein, C. Karako-Argaman, C. A. McPhee, T. Pennucci, M. S. E. Roberts, K. Stovall and J. van Leeuwen, *ApJ* **763** (2013) 81.
10. P. Lazarus, A. Brazier, J. W. T. Hessels, C. Karako-Argaman, V. M. Kaspi, R. Lynch, E. Madsen, C. Patel, S. M. Ransom, P. Scholz, J. Swiggum, W. W. Zhu, B. Allen, S. Bogdanov, F. Camilo, F. Cardoso, S. Chatterjee, J. M. Cordes, F. Crawford, J. S. Deneva, R. Ferdman, P. C. C. Freire, F. A. Jenet, B. Knispel, K. J. Lee, J. van Leeuwen, D. R. Lorimer, A. G. Lyne, M. A. McLaughlin, X. Siemens, L. G. Spitler, I. H. Stairs, K. Stovall and A. Venkataraman, *ArXiv/1504.02294* (2015).
11. C.-A. Faucher-Giguère and V. M. Kaspi, *ApJ* **643** (2006) 332.
12. A. G. Lyne and D. R. Lorimer, *Nature* **369** (1994) 127.
13. B. Hansen and E. S. Phinney, *MNRAS* **291** (1997) 569.
14. G. Hobbs, D. R. Lorimer, A. G. Lyne and M. Kramer, *MNRAS* **360** (2005) 974.
15. S. D. Bates, D. R. Lorimer, A. Rane and J. Swiggum, *MNRAS* **439** (2014) 2893.
16. M. D. Young, R. N. Manchester and S. Johnston, *Nature* **400** (1999) 848.
17. J. W. T. Hessels, S. M. Ransom, I. H. Stairs, P. C. C. Freire, V. M. Kaspi and F. Camilo, *Science* **311** (2006) 1901.
18. P. Goldreich and W. H. Julian, *ApJ* **157** (1969) 869.
19. A. Spitkovsky, *ApJL* **648** (2006) L51.
20. M. A. Livingstone, V. M. Kaspi, F. P. Gavriil, R. N. Manchester, E. V. G. Gotthelf and L. Kuiper, *ApSS* **308** (2007) 317.
21. V. M. Kaspi, M. S. E. Roberts, G. Vasisht, E. V. Gotthelf, M. Pivovarov and N. Kawai, *ApJ* **560** (2001) 371.
22. D. H. Clark and F. R. Stephenson, *The Historical Supernovae* (Pergamon, Oxford, 1977).
23. M. A. Livingstone, V. M. Kaspi, E. V. Gotthelf and L. Kuiper, *ApJ* **647** (2006) 1286.
24. D. B. Melrose, Coherent radio emission from pulsars., in *Pulsars as Physics Laboratories*, eds. J. M. Shull and H. A. Thronson (1993), pp. 105–115.
25. D. B. Melrose, *J. Astrophys. Astr.* **16** (1995) 137.
26. R. Beck, *Philos. Trans. Roy. Soc. London A* **358** (2000) 777.
27. V. M. Kaspi, M. S. E. Roberts and A. K. Harding, Isolated neutron stars pp. 279–339.
28. B. M. Gaensler and P. O. Slane, *Ann. Rev. Astr. Ap.* **44** (2006) 17.
29. P. A. Caraveo, *araa* **52** (2014) 211.

30. D. Bhattacharya and E. P. J. van den Heuvel, *Phys. Rep.* **203** (1991) 1.
31. E. S. Phinney and S. R. Kulkarni, *Ann. Rev. Astr. Ap.* **32** (1994) 591.
32. T. M. Tauris and E. P. J. van den Heuvel, Formation and evolution of compact stellar X-ray sources (Compact stellar X-ray sources, 2006), pp. 623–665.
33. D. R. Lorimer, *Living Reviews in Relativity* (2008) <http://www.livingreviews.org/lrr-2008-8>.
34. D. C. Backer, S. R. Kulkarni, C. Heiles, M. M. Davis and W. M. Goss, *Nature* **300** (1982) 615.
35. A. S. Fruchter, D. R. Stinebring and J. H. Taylor, *Nature* **333** (1988) 237.
36. B. W. Stappers, M. Bailes, A. G. Lyne, R. N. Manchester, N. D’Amico, T. M. Tauris, D. R. Lorimer, S. Johnston and J. S. Sandhu, *ApJ* **465** (1996) L119.
37. A. M. Archibald, I. H. Stairs, S. M. Ransom, V. M. Kaspi, V. I. Kondratiev, D. R. Lorimer, M. A. McLaughlin, J. Boyles, J. W. T. Hessels, R. Lynch, J. van Leeuwen, M. S. E. Roberts, F. Jenet, D. J. Champion, R. Rosen, B. N. Barlow, B. H. Dunlap and R. A. Remillard, *Science* **324** (2009) 1411.
38. D. R. Lorimer, A. J. Faulkner, A. G. Lyne, R. N. Manchester, M. Kramer, M. A. McLaughlin, G. Hobbs, A. Possenti, I. H. Stairs, F. Camilo, M. Burgay, N. D’Amico, A. Corongiu and F. Crawford, *MNRAS* **372** (2006) 777.
39. J. P. W. Verbiest, M. Bailes, W. A. Coles, G. B. Hobbs, W. van Straten, D. J. Champion, F. A. Jenet, R. N. Manchester, N. D. R. Bhat, J. M. Sarkissian, D. Yardley, S. Burke-Spolaor, A. W. Hotan and X. P. You, *MNRAS* **400** (2009) 951.
40. D. J. Champion, S. M. Ransom, P. Lazarus, F. Camilo, C. Bassa, V. M. Kaspi, D. J. Nice, P. C. C. Freire, I. H. Stairs, J. van Leeuwen, B. W. Stappers, J. M. Cordes, J. W. T. Hessels, D. R. Lorimer, Z. Arzoumanian, D. C. Backer, N. D. R. Bhat, S. Chatterjee, I. Cognard, J. S. Deneva, C.-A. Faucher-Giguère, B. M. Gaensler, J. Han, F. A. Jenet, L. Kasian, V. I. Kondratiev, M. Kramer, J. Lazio, M. A. McLaughlin, A. Venkataraman and W. Vlemmings, *Science* **320** (2008) 1309.
41. P. C. C. Freire, C. G. Bassa, N. Wex, I. H. Stairs, D. J. Champion, S. M. Ransom, P. Lazarus, V. M. Kaspi, J. W. T. Hessels, M. Kramer, J. M. Cordes, J. P. W. Verbiest, P. Podsiadlowski, D. J. Nice, J. S. Deneva, D. R. Lorimer, B. W. Stappers, M. A. McLaughlin and F. Camilo, *MNRAS* **412** (2011) 2763.
42. S. M. Ransom, I. H. Stairs, A. M. Archibald, J. W. T. Hessels, D. L. Kaplan, M. H. van Kerkwijk, J. Boyles, A. T. Deller, S. Chatterjee, A. Schechtman-Rook, A. Berndsen, R. S. Lynch, D. R. Lorimer, C. Karako-Argaman, V. M. Kaspi, V. I. Kondratiev, M. A. McLaughlin, J. van Leeuwen, R. Rosen, M. S. E. Roberts and K. Stovall, *Nature* **505** (2014) 520.
43. T. M. Tauris and E. P. J. van den Heuvel, *ApJL* **781** (2014) L13.
44. J. S. Deneva, K. Stovall, M. A. McLaughlin, S. D. Bates, P. C. C. Freire, J. G. Martinez, F. Jenet and M. Bagchi, *ApJ* **775** (2013) 51.
45. B. Knispel, A. G. Lyne, B. W. Stappers, P. C. C. Freire, P. Lazarus, B. Allen, C. Aulbert, O. Bock, S. Bogdanov, A. Brazier, F. Camilo, F. Cardoso, S. Chatterjee, J. M. Cordes, F. Crawford, J. S. Deneva, H.-B. Eggenstein, H. Fehrmann, R. Ferdman, J. W. T. Hessels, F. A. Jenet, C. Karako-Argaman, V. M. Kaspi, J. van Leeuwen, D. R. Lorimer, R. Lynch, B. Machenschalk, E. Madsen, M. A. McLaughlin, C. Patel, S. M. Ransom, P. Scholz, X. Siemens, L. G. Spitler, I. H. Stairs, K. Stovall, J. K. Swiggum, A. Venkataraman, R. S. Wharton and W. W. Zhu, *ArXiv/1504.03684* (2015).
46. P. C. C. Freire and T. M. Tauris, *MNRAS* **438** (2014) L86.
47. J. Antoniadis, *ApJ* **797** (2014) L24.
48. A. Papitto, C. Ferrigno, E. Bozzo, N. Rea, L. Pavan, L. Burderi, M. Burgay, S. Cam-

- pana, T. di Salvo, M. Falanga, M. D. Filipović, P. C. C. Freire, J. W. T. Hessels, A. Possenti, S. M. Ransom, A. Riggio, P. Romano, J. M. Sarkissian, I. H. Stairs, L. Stella, D. F. Torres, M. H. Wieringa and G. F. Wong, *Nature* **501** (2013) 517.
49. B. W. Stappers, A. M. Archibald, J. W. T. Hessels, C. G. Bassa, S. Bogdanov, G. H. Janssen, V. M. Kaspi, A. G. Lyne, A. Patruno, S. Tendulkar, A. B. Hill and T. Glanzman, *ApJ* **790** (2014) 39.
 50. S. P. Tendulkar, C. Yang, H. An, V. M. Kaspi, A. M. Archibald, C. Bassa, E. Bellm, S. Bogdanov, F. A. Harrison, J. W. T. Hessels, G. H. Janssen, A. G. Lyne, A. Patruno, B. Stappers, D. Stern, J. A. Tomsick, S. E. Boggs, D. Chakrabarty, F. E. Christensen, W. W. Craig, C. A. Hailey and W. Zhang, *ApJ* **791** (2014) 77.
 51. S. Bogdanov, A. Patruno, A. M. Archibald, C. Bassa, J. W. T. Hessels, G. H. Janssen and B. W. Stappers, *ApJ* **789** (2014) 40.
 52. S. Johnston, R. N. Manchester, A. G. Lyne, M. Bailes, V. M. Kaspi, G. Qiao and N. D'Amico, *ApJ* **387** (1992) L37.
 53. V. M. Kaspi, S. Johnston, J. F. Bell, R. N. Manchester, M. Bailes, M. Bessell, A. G. Lyne and N. D'Amico, *ApJ* **423** (1994) L43.
 54. I. H. Stairs, R. N. Manchester, A. G. Lyne, V. M. Kaspi, F. Camilo, J. F. Bell, N. D'Amico, M. Kramer, F. Crawford, D. J. Morris, N. P. F. McKay, S. L. Lumsden, L. E. Tacconi-Garman, R. D. Cannon, N. C. Hambly and P. R. Wood, *MNRAS* **325** (2001) 979.
 55. D. Lai, L. Bildsten and V. M. Kaspi, *ApJ* **452** (1995) 819.
 56. V. M. Kaspi, M. Bailes, R. N. Manchester, B. W. Stappers and J. F. Bell, *Nature* **381** (1996) 584.
 57. N. Wex, *MNRAS* **298** (1998) 67.
 58. E. C. Madsen, I. H. Stairs, M. Kramer, F. Camilo, G. B. Hobbs, G. H. Janssen, A. G. Lyne, R. N. Manchester, A. Possenti and B. W. Stappers, *MNRAS* **425** (2012) 2378.
 59. S. Johnston, L. Ball, N. Wang and R. N. Manchester, *MNRAS* **358** (2005) 1069.
 60. V. M. Kaspi, T. Tauris and R. N. Manchester, *ApJ* **459** (1996) 717.
 61. A. A. Abdo, et al., *ApJL* **736** (2011) L11.
 62. HESS run/Collaboration, *A&A* **551** (2013) A94.
 63. I. F. Mirabel, *Science* **335** (2012) 175.
 64. V. M. Kaspi, *Proceedings of the National Academy of Science* **107** (2010) 7147.
 65. E. P. Mazets, S. V. Golenetskii and Y. A. Gur'yan, *Sov. Astron. Lett.* **5** (1979) 343.
 66. E. P. Mazets, S. V. Golenetskii, V. N. Ilinskii, R. L. Apetkar and Y. A. Guryan, *Nature* **282** (1979) 587.
 67. S. A. Olausen and V. M. Kaspi, *ApJS* **212** (2014) 6.
 68. S. Mereghetti, J. A. Pons and A. Melatos, *Space Sciences Review, arXiv/1503.06313* (2015).
 69. K. Hurley, S. E. Boggs, D. M. Smith, R. C. Duncan, R. Lin, A. Zoglauer, S. Krucker, G. Hurford, H. Hudson, C. Wigger, W. Hajdas, C. Thompson, I. Mitrofanov, A. Sanin, W. Boynton, C. Fellows, A. von Kienlin, G. Lichti, A. Rau and T. Cline, *Nature* **434** (2005) 1098.
 70. D. M. Palmer, S. Barthelmy, N. Gehrels, R. M. Kippen, T. Cayton, C. Kouveliotou, D. Eichler, R. A. M. J. Wijers, P. M. Woods, J. Granot, Y. E. Lyubarsky, E. Ramirez-Ruiz, L. Barbier, M. Chester, J. Cummings, E. E. Fenimore, M. H. Finger, B. M. Gaensler, D. Hullinger, H. Krimm, C. B. Markwardt, J. A. Nousek, A. Parsons, S. Patel, T. Sakamoto, G. Sato, M. Suzuki and J. Tueller, *Nature* **434** (2005) 1107.
 71. M. P. Muno, J. S. Clark, P. A. Crowther, S. M. Dougherty, R. de Grijs, C. Law, S. L. W. McMillan, M. R. Morris, I. Negueruela, D. Pooley, S. Portegies Zwart and F. Yusef-Zadeh, *ApJ* **636** (2006) L41.

72. S. Mereghetti, G. L. Israel and L. Stella, *MNRAS* **296** (1998) 689.
73. T. Damour and J. H. Taylor, *Phys. Rev. D* **45** (1992) 1840.
74. C. Thompson and R. C. Duncan, *MNRAS* **275** (1995) 255.
75. C. Thompson and R. C. Duncan, *ApJ* **473** (1996) 322.
76. P. Goldreich and A. Reisenegger, *ApJ* **395** (1992) 250.
77. C. Kouveliotou, S. Dieters, T. Strohmayer, J. van Paradijs, G. J. Fishman, C. A. Meegan, K. Hurley, J. Kommers, I. Smith, D. Frail and T. Murakami, *Nature* **393** (1998) 235.
78. F. P. Gavriil, V. M. Kaspi and P. M. Woods, *Nature* **419** (2002) 142.
79. V. M. Kaspi, F. P. Gavriil, P. M. Woods, J. B. Jensen, M. S. E. Roberts and D. Chakrabarty, *ApJ* **588** (2003) L93.
80. C. Thompson, M. Lyutikov and S. R. Kulkarni, *ApJ* **574** (2002) 332.
81. A. M. Beloborodov and C. Thompson, *ApJ* **657** (2007) 967.
82. Y. Lyubarsky, D. Eichler and C. Thompson, *ApJ* **580** (2002) L69.
83. C. Kouveliotou, D. Eichler, P. M. Woods, Y. Lyubarsky, S. K. Patel, E. Göğüş, M. van der Klis, A. Tennant, S. Wachter and K. Hurley, *ApJ* **596** (2003) L79.
84. P. Scholz, V. M. Kaspi and A. Cumming, *ApJ* **786** (2014) 62.
85. L. Kuiper, W. Hermsen and M. Mendez, *ApJ* **613** (2004) 1173.
86. L. Kuiper, W. Hermsen, P. den Hartog and W. Collmar, *ApJ* **645** (2006) 556.
87. A. M. Beloborodov, *ApJ* **777** (2013) 114.
88. R. Dib, V. M. Kaspi and F. P. Gavriil, *ApJ* **673** (2008) 1044.
89. P. W. Anderson and N. Itoh, *Nature* **256** (1975) 25.
90. M. A. Alpar, K. S. Cheng and D. Pines, *ApJ* **346** (1989) 823.
91. R. Dib and V. M. Kaspi, *ApJ* **784** (2014) 37.
92. R. F. Archibald, V. M. Kaspi, C.-Y. Ng, K. N. Gourgouliatos, D. Tsang, P. Scholz, A. P. Beardmore, N. Gehrels and J. A. Kennea, *Nature* **497** (2013) 591.
93. N. Rea, P. Esposito, R. Turolla, G. L. Israel, S. Zane, L. Stella, S. Mereghetti, A. Tiengo, D. Götz, E. Göğüş and C. Kouveliotou, *Science* **330** (2010) 944.
94. F. P. Gavriil, M. E. Gonzalez, E. V. Gotthelf, V. M. Kaspi, M. A. Livingstone and P. M. Woods, *Science* **319** (2008) 1802.
95. M. A. Livingstone, C.-Y. Ng, V. M. Kaspi, F. P. Gavriil and E. V. Gotthelf, *ApJ* **730** (2011) 66.
96. R. Perna and J. A. Pons, *ApJ* **727** (February 2011) L51.
97. D. Viganò, N. Rea, J. A. Pons, R. Perna, D. N. Aguilera and J. A. Miralles, *MNRAS* **434** (September 2013) 123.
98. F. Camilo, S. M. Ransom, J. P. Halpern, J. Reynolds, D. J. Helfand, N. Zimmerman and J. Sarkissian, *Nature* **442** (2006) 892.
99. F. Camilo, S. M. Ransom, J. P. Halpern and J. Reynolds, *ApJ* **666** (2007) L93.
100. L. Levin, M. Bailes, S. Bates, N. D. R. Bhat, M. Burgay, S. Burke-Spolaor, N. D'Amico, S. Johnston, M. Keith, M. Kramer, S. Milia, A. Possenti, N. Rea, B. Stappers and W. van Straten, *ApJ* (2010).
101. R. P. Eatough, H. Falcke, R. Karuppusamy, K. J. Lee, D. J. Champion, E. F. Keane, G. Desvignes, D. H. F. M. Schnitzeler, L. G. Spitler, M. Kramer, B. Klein, C. Bassa, G. C. Bower, A. Brunthaler, I. Cognard, A. T. Deller, P. B. Demorest, P. C. C. Freire, A. Kraus, A. G. Lyne, A. Noutsos, B. Stappers and N. Wex, *Nature* **501** (2013) 391.
102. K. Mori, E. V. Gotthelf, S. Zhang, H. An, F. K. Baganoff, N. M. Barrière, A. M. Beloborodov, S. E. Boggs, F. E. Christensen, W. W. Craig, F. Dufour, B. W. Grefenstette, C. J. Hailey, F. A. Harrison, J. Hong, V. M. Kaspi, J. A. Kennea, K. K. Madsen, C. B. Markwardt, M. Nynka, D. Stern, J. A. Tomsick and W. W. Zhang, *ApJ* **770** (2013) L23.

103. N. Rea, P. Esposito, J. A. Pons, R. Turolla, D. F. Torres, G. L. Israel, A. Possenti, M. Burgay, D. Vigano', R. Perna, L. Stella, G. Ponti, F. Baganoff, D. Haggard, A. Pappitto, A. Camero-Arranz, S. Zane, A. Minter, S. Mereghetti, A. Tiengo, R. Schoedel, M. Feroci, R. Mignani and D. Gotz, *ApJL* **775** (2013) L34.
104. R. M. Shannon and S. Johnston, *MNRAS* **435** (2013) L29.
105. V. M. Kaspi, R. F. Archibald, V. Bhlerao, F. Dufour, E. V. Gotthelf, H. An, M. Bachetti, A. M. Beloborodov, S. E. Boggs, F. E. Christensen, W. W. Craig, B. W. Grefenstette, C. J. Hailey, F. A. Harrison, J. A. Kennea, C. Kouveliotou, K. K. Madsen, K. Mori, C. B. Markwardt, D. Stern, J. K. Vogel and W. W. Zhang, *ApJ* **786** (2014) 84.
106. F. Haberl, *ApJS* (2007) 73.
107. D. L. Kaplan and M. H. van Kerkwijk, *ApJ* **705** (2009) 798.
108. E. F. Keane and M. Kramer, *MNRAS* **391** (2008) 2009.
109. D. L. Kaplan and M. H. van Kerkwijk, *ApJ* **635** (2005) L65.
110. J. A. Pons, B. Link, J. A. Miralles and U. Geppert, *Phys. Rev. Lett.* **98** (2007) 071101.
111. W. Zhu, V. M. Kaspi, M. E. Gonzalez and A. G. Lyne, *ApJ* **704** (2009) 1321.
112. D. N. Aguilera, J. A. Pons and J. A. Miralles, *ApJ* **673** (2008) L167.
113. J. A. Pons, J. A. Miralles and U. Geppert, **496** (2009) 207.
114. K. N. Gourgouliatos and A. Cumming, *MNRAS* **438** (February 2014) 1618.
115. G. G. Pavlov, V. E. Zavlin, B. Aschenbach, J. Truemper and D. Sanwal, *ApJ* **531** (1999) L53.
116. D. Chakrabarty, M. J. Pivovarov, L. E. Hernquist, J. S. Heyl and R. Narayan, *ApJ* **548** (2001) 800.
117. S. Mereghetti, A. Tiengo and G. L. Israel, *ApJ* **569** (2002) 275.
118. G. G. Pavlov and G. J. M. Luna, *ApJ* **703** (2009) 910.
119. E. V. Gotthelf, J. P. Halpern and F. D. Seward, *ApJ* **627** (2005) 390.
120. J. P. Halpern, E. V. Gotthelf, F. Camilo and F. D. Seward, *ApJ* **665** (2007) 1304.
121. J. P. Halpern and E. V. Gotthelf, *ApJ* **709** (2010) 436.
122. V. E. Zavlin, G. G. Pavlov, D. Sanwal and J. Trümper, *ApJ* **540** (2000) L25.
123. G. G. Pavlov, V. E. Zavlin, D. Sanwal and J. Trümper, *ApJ* **569** (2002) L95.
124. E. V. Gotthelf, J. P. Halpern and J. Alford, *ApJ* **765** (2013) 58.
125. E. V. Gotthelf and J. P. Halpern, *ApJ* **695** (2009) L35.
126. M. A. McLaughlin, A. G. Lyne, D. R. Lorimer, M. Kramer, A. J. Faulkner, R. N. Manchester, J. M. Cordes, F. Camilo, A. Possenti, I. H. Stairs, G. Hobbs, N. D'Amico, M. Burgay and J. T. O'Brien, *Nature* **439** (2006) 817.
127. P. Weltevrede, B. W. Stappers, J. M. Rankin and G. A. E. Wright, *ApJ* **645** (2006) L149.
128. E. F. Keane, M. Kramer, A. G. Lyne, B. W. Stappers and M. A. McLaughlin, *MNRAS* **415** (2011) 3065.
129. E. Petroff, E. F. Keane, E. D. Barr, J. E. Reynolds, J. Sarkissian, P. G. Edwards, J. Stevens, C. Brem, A. Jameson, S. Burke-Spolaor, S. Johnston, N. D. R. Bhat, P. Chandra, S. Kudale and S. Bhandari, *ArXiv e-prints/1504.02165* (2015).
130. D. R. Lorimer, M. Bailes, M. A. McLaughlin, D. J. Narkevic and F. Crawford, *Science* **318** (2007) 777.
131. D. Thornton, B. Stappers, M. Bailes, B. Barsdell, S. Bates, N. D. R. Bhat, M. Burgay, S. Burke-Spolaor, D. J. Champion, P. Coster, N. D'Amico, A. Jameson, S. Johnston, M. Keith, M. Kramer, L. Levin, S. Milia, C. Ng, A. Possenti and W. van Straten, *Science* **341** (2013) 53.
132. L. G. Spitler, J. M. Cordes, J. W. T. Hessels, D. R. Lorimer, M. A. McLaughlin, S. Chatterjee, F. Crawford, J. S. Deneva, V. M. Kaspi, R. S. Wharton, B. Allen,

- S. Bogdanov, A. Brazier, F. Camilo, P. C. C. Freire, F. A. Jenet, C. Karako-Argaman, B. Knispel, P. Lazarus, K. J. Lee, J. van Leeuwen, R. Lynch, S. M. Ransom, P. Scholz, X. Siemens, I. H. Stairs, K. Stovall, J. K. Swiggum, A. Venkataraman, W. W. Zhu, C. Aulbert and H. Fehrmann, *ApJ* **790** (2014) 101.
133. E. Petroff, M. Bailes, E. D. Barr, B. R. Barsdell, N. D. R. Bhat, F. Bian, S. Burke-Spolaor, M. Caleb, D. Champion, P. Chandra, G. Da Costa, C. Delvaux, C. Flynn, N. Gehrels, J. Greiner, A. Jameson, S. Johnston, M. M. Kasliwal, E. F. Keane, S. Keller, J. Kocz, M. Kramer, G. Leloudas, D. Malesani, J. S. Mulchaey, C. Ng, E. O. Ofek, D. A. Perley, A. Possenti, B. P. Schmidt, Y. Shen, B. Stappers, P. Tisserand, W. van Straten and C. Wolf, *MNRAS* **447** (2015) 246.
134. E. Petroff, W. van Straten, S. Johnston, M. Bailes, E. D. Barr, S. D. Bates, N. D. R. Bhat, M. Burgay, S. Burke-Spolaor, D. Champion, P. Coster, C. Flynn, E. F. Keane, M. J. Keith, M. Kramer, L. Levin, C. Ng, A. Possenti, B. W. Stappers, C. Tiburzi and D. Thornton, *ApJ* **789** (2014) L26.
135. C. M. Will, *Living Reviews in Relativity* **17** (2014) 4.
136. S. Blatt, A. D. Ludlow, G. K. Campbell, J. W. Thomsen, T. Zelevinsky, M. M. Boyd, J. Ye, X. Baillard, M. Fouché, R. Le Targat, A. Bruschi, P. Lemonde, M. Takamoto, F.-L. Hong, H. Katori and V. V. Flambaum, *Phys. Rev. Lett.* **100** (2008) 140801.
137. A. Ivanchik, P. Petitjean, D. Varshalovich, B. Aracil, R. Srianand, H. Chand, C. Ledoux and P. Boissé, *A&A* **440** (2005) 45.
138. F. Hofmann, J. Müller and L. Biskupek, *A&A* **522** (2010) L5.
139. P. C. C. Freire, N. Wex, G. Esposito-Farèse, J. P. W. Verbiest, M. Bailes, B. A. Jacoby, M. Kramer, I. H. Stairs, J. Antoniadis and G. H. Janssen, *MNRAS* **423** (2012) 3328.
140. N. Wex, in the Brumberg Festschrift, edited by S. M. Kopeikin, Gruyter, Berlin, *ArXiv/1402.5594* (2014).
141. I. H. Stairs, A. J. Faulkner, A. G. Lyne, M. Kramer, D. R. Lorimer, M. A. McLaughlin, R. N. Manchester, G. B. Hobbs, F. Camilo, A. Possenti, M. Burgay, N. D'Amico, P. C. C. Freire, P. C. Gregory and N. Wex, *ApJ* **632** (2005) 1060.
142. M. Kramer and et al., *Phys. Rev. D* (2015) to be submitted.
143. J. Antoniadis, P. C. C. Freire, N. Wex, T. M. Tauris, R. S. Lynch, M. H. van Kerkwijk, M. Kramer, C. Bassa, V. S. Dhillon, T. Driebe, J. W. T. Hessels, V. M. Kaspi, V. I. Kondratiev, N. Langer, T. R. Marsh, M. A. McLaughlin, T. T. Pennucci, S. M. Ransom, I. H. Stairs, J. van Leeuwen, J. P. W. Verbiest and D. G. Whelan, *Science* **340** (2013) 448.
144. C. W. F. Everitt, D. B. Debra, B. W. Parkinson, J. P. Turneare, J. W. Conklin, M. I. Heifetz, G. M. Keiser, A. S. Silbergleit, T. Holmes, J. Kolodziejczak, M. Al-Meshari, J. C. Mester, B. Muhlfelder, V. G. Solomonik, K. Stahl, P. W. Worden, Jr., W. Bencze, S. Buchman, B. Clarke, A. Al-Jadaan, H. Al-Jibreen, J. Li, J. A. Lipa, J. M. Lockhart, B. Al-Suwaidan, M. Taber and S. Wang, *Phys. Rev. Lett.* **106** (2011) 221101.
145. M. Kramer, *ApJ* **509** (1998) 856.
146. R. P. Breton, V. M. Kaspi, M. Kramer, M. A. McLaughlin, M. Lyutikov, S. M. Ransom, I. H. Stairs, R. D. Ferdman, F. Camilo and A. Possenti, *Science* **321** (2008) 104.
147. J. M. Lattimer and A. W. Steiner, *ApJ* **784** (2014) 123.
148. P. B. Demorest, T. Pennucci, S. M. Ransom, M. S. E. Roberts and J. W. T. Hessels, *Nature* **467** (2010) 1081.
149. S. Guillot, M. Servillat, N. A. Webb and R. E. Rutledge, *ApJ* **772** (July 2013) 7.
150. L. Shao and N. Wex, *Class. Quant Grav.* **30** (2013) 165020.

151. L. Shao and N. Wex, *Class. Quant Grav.* **29** (2012) 215018.
152. L. Shao, R. N. Caballero, M. Kramer, N. Wex, D. J. Champion and A. Jessner, *Class. Quant Grav.* **30** (2013) 165019.
153. J. Alsing, E. Berti, C. M. Will and H. Zaglauer, *Phys. Rev. D* **85** (2012) 064041.
154. K. Yagi, D. Blas, E. Barausse and N. Yunes, *Phys. Rev. D* **89** (2014) 084067.
155. K. Liu, N. Wex, M. Kramer, J. M. Cordes and T. J. W. Lazio, *ApJ* **747** (2012) 1.
156. V. M. Kaspi, A. G. Lyne, R. N. Manchester, F. Crawford, F. Camilo, J. F. Bell, N. D'Amico, I. H. Stairs, N. P. F. McKay, D. J. Morris and A. Possenti, *ApJ* **543** (2000) 321.
157. R. A. Hulse and J. H. Taylor, *ApJ* **195** (1975) L51.
158. D. R. Lorimer and M. Kramer, *Handbook of Pulsar Astronomy* (Cambridge University Press, 2005).
159. J. M. Weisberg, D. J. Nice and J. H. Taylor, *ApJ* **722** (2010) 1030.
160. T. Damour and J. H. Taylor, *ApJ* **366** (1991) 501.
161. M. Burgay, N. D'Amico, A. Possenti, R. N. Manchester, A. G. Lyne, B. C. Joshi, M. A. McLaughlin, M. Kramer, J. M. Sarkissian, F. Camilo, V. Kalogera, C. Kim and D. R. Lorimer, *Nature* **426** (2003) 531.
162. A. G. Lyne, M. Burgay, M. Kramer, A. Possenti, R. N. Manchester, F. Camilo, M. A. McLaughlin, D. R. Lorimer, N. D'Amico, B. C. Joshi, J. Reynolds and P. C. C. Freire, *Science* **303** (2004) 1153.
163. M. Kramer, I. H. Stairs, R. N. Manchester, M. A. McLaughlin, A. G. Lyne, R. D. Ferdman, M. Burgay, D. R. Lorimer, A. Possenti, N. D'Amico, J. M. Sarkissian, G. B. Hobbs, J. E. Reynolds, P. C. C. Freire and F. Camilo, *Science* **314** (2006) 97.
164. M. Kramer and I. H. Stairs, *Ann. Rev. Astr. Ap.* **46** (2008) 541.
165. M. Kramer and N. Wex, *Classical and Quantum Gravity* **26** (2009) 073001.
166. T. Damour and N. Deruelle, *Ann. Inst. H. Poincaré (Physique Théorique)* **44** (1986) 263.
167. G. Boerner, J. Ehlers and E. Rudolph, *A&A* **44** (1975) 417.
168. T. Damour and R. Ruffini, *Academie des Sciences Paris Comptes Rendus Ser. Scie. Math.* **279** (1974) 971.
169. R. D. Ferdman, I. H. Stairs, M. Kramer, R. P. Breton, M. A. McLaughlin, P. C. C. Freire, A. Possenti, B. W. Stappers, V. M. Kaspi, R. N. Manchester and A. G. Lyne, *ApJ* **767** (2013) 85.
170. M. Burgay, A. Possenti, R. N. Manchester, M. Kramer, M. A. McLaughlin, D. R. Lorimer, I. H. Stairs, B. C. Joshi, A. G. Lyne, F. Camilo, N. D'Amico, P. C. C. Freire, J. M. Sarkissian, A. W. Hotan and G. B. Hobbs, *ApJ* **624** (2005) L113.
171. B. B. P. Perera, M. A. McLaughlin, M. Kramer, I. H. Stairs, R. D. Ferdman, P. C. C. Freire, A. Possenti, R. P. Breton, R. N. Manchester, M. Burgay, A. G. Lyne and F. Camilo, *ApJ* **721** (2010) 1193.
172. T. Damour and G. Esposito-Farese, *Phys. Rev. D* **54** (1996) 1474.
173. B. Bertotti, L. Iess and P. Tortora, *Nature* **425** (2003) 374.
174. J. D. Bekenstein, *Phys. Rev. D* **70** (2004) 083509.
175. R. W. Hellings and G. S. Downs, *ApJ* **265** (1983) L39.
176. G. H. Janssen, G. Hobbs, M. McLaughlin, C. G. Bassa, A. T. Deller, M. Kramer, K. J. Lee, C. M. F. Mingarelli, P. A. Rosado, S. Sanidas, A. Sesana, L. Shao, I. H. Stairs, B. W. Stappers and J. P. W. Verbiest, *ArXiv/1501.00127* (2015).
177. R. N. Manchester and IPTA, *Class. Quant Grav.* **30** (2013) 224010.
178. R. M. Shannon, V. Ravi, W. A. Coles, G. Hobbs, M. J. Keith, R. N. Manchester, J. S. B. Wyithe, M. Bailes, N. D. R. Bhat, S. Burke-Spolaor, J. Khoo, Y. Levin, S. Osłowski, J. M. Sarkissian, W. van Straten, J. P. W. Verbiest and J.-B. Wang,

- Science* **342** (2013) 334.
179. A. Sesana, A. Vecchio and C. N. Colacino, *MNRAS* **390** (2008) 192.
 180. A. Sesana and A. Vecchio, *Class. Quant Grav.* **27** (2010) 084016.
 181. A. Sesana, *MNRAS* **433** (2013) L1.
 182. A. Sesana, *Astrophysics and Space Science Proceedings* **40** (2015) 147.
 183. C. Roedig, M. Dotti, A. Sesana, J. Cuadra and M. Colpi, *MNRAS* **415** (2011) 3033.
 184. C. Roedig and A. Sesana, *Journal of Physics Conference Series* **363** (2012) 012035.
 185. L. Sampson, N. J. Cornish and S. T. McWilliams, *ArXiv/1503.02662* (2015).
 186. K. J. Lee, N. Wex, M. Kramer, B. W. Stappers, C. G. Bassa, G. H. Janssen, R. Karuppusamy and R. Smits, *MNRAS* **414** (2011) 3251.
 187. C. M. F. Mingarelli, T. Sidery, I. Mandel and A. Vecchio, *Phys. Rev. D* **88** (2013) 062005.
 188. D. J. Champion, G. B. Hobbs, R. N. Manchester, R. T. Edwards, D. C. Backer, M. Bailes, N. D. R. Bhat, S. Burke-Spolaor, W. Coles, P. B. Demorest, R. D. Ferdman, W. M. Folkner, A. W. Hotan, M. Kramer, A. N. Lommen, D. J. Nice, M. B. Purver, J. M. Sarkissian, I. H. Stairs, W. van Straten, J. P. W. Verbiest and D. R. B. Yardley, *ApJ* **720** (2010) L201.
 189. K. J. Lee, F. A. Jenet and R. H. Price, *ApJ* **685** (2008) 1304.
 190. S. J. Chamberlin and X. Siemens, *Phys. Rev. D* **85** (2012) 082001.
 191. C. M. F. Mingarelli, K. Grover, T. Sidery, R. J. E. Smith and A. Vecchio, *Physical Review Letters* **109** (2012) 081104.
 192. K. Lee, F. A. Jenet, R. H. Price, N. Wex and M. Kramer, *ApJ* **722** (2010) 1589.
 193. T. Damour and G. Esposito-Farèse, *Phys. Rev. D* **58** (1998) 1.
 194. N. Wex and S. Kopeikin, *ApJ* **513** (1999) 388.
 195. M. Kramer, D. C. Backer, J. M. Cordes, T. J. W. Lazio, B. W. Stappers and S. Johnston, *New Astronomy Reviews* **48** (2004) 993.
 196. K. Liu, R. P. Eatough, N. Wex and M. Kramer, *MNRAS* (2014).
 197. R. Nan, D. Li, C. Jin, Q. Wang, L. Zhu, W. Zhu, H. Zhang, Y. Yue and L. Qian, *International Journal of Modern Physics D* **20** (2011) 989.
 198. E. Pfahl and A. Loeb, *ApJ* **615** (2004) 253.
 199. G. C. Bower, A. Deller, P. Demorest, A. Brunthaler, R. Eatough, H. Falcke, M. Kramer, K. J. Lee and L. Spitler, *ApJ* **780** (2014) L2.
 200. L. G. Spitler, K. J. Lee, R. P. Eatough, M. Kramer, R. Karuppusamy, C. G. Bassa, I. Cognard, G. Desvignes, A. G. Lyne, B. W. Stappers, G. C. Bower, J. M. Cordes, D. J. Champion and H. Falcke, *ApJ* **780** (2014) L3.
 201. R. S. Lynch, R. F. Archibald, V. M. Kaspi and P. Scholz, *ApJ*.
 202. R. S. Wharton, S. Chatterjee, J. M. Cordes, J. S. Deneva and T. J. W. Lazio, *ApJ* **753** (2012) 108.
 203. A. M. Ghez, S. Salim, N. N. Weinberg, J. R. Lu, T. Do, J. K. Dunn, K. Matthews, M. R. Morris, S. Yelda, E. E. Becklin, T. Kremenek, M. Milosavljevic and J. Naiman, *ApJ* **689** (December 2008) 1044.
 204. S. Gillessen, F. Eisenhauer, T. K. Fritz, H. Bartko, K. Dodds-Eden, O. Pfuhl, T. Ott and R. Genzel, *ApJ* **707** (2009) L114.
 205. H. Falcke and S. B. Markoff, *Class. Quant Grav.* **30** (2013) 244003.
 206. D. Psaltis, F. Özel and D. Chakrabarty, *ApJ* **787** (2014) 136.
 207. J. M. Lattimer, *General Relativity and Gravitation* **46** (2014) 1713.
 208. P. Podsiadlowski, J. D. M. Dewi, P. Lesaffre, J. C. Miller, W. G. Newton and J. R. Stone, *MNRAS* **361** (2005) 1243.
 209. T. M. Tauris, N. Langer, T. J. Moriya, P. Podsiadlowski, S.-C. Yoon and S. I. Blinnikov, *ApJ* **778** (2013) L23.

210. J. M. Lattimer and B. F. Schutz, *ApJ* **629** (2005) 979.
211. I. A. Morrison, T. W. Baumgarte, S. L. Shapiro and V. R. Pandharipande, *ApJ* **617** (2004) L135.
212. M. Bejger, T. Bulik and P. Haensel, *MNRAS* **364** (2005) 635.
213. A. Loeb, Y. Shvartzvald and D. Maoz, *MNRAS* **439** (2014) L46.
214. J. Luan and P. Goldreich, *ApJL* **785** (2014) L26.
215. B. Dennison, *MNRAS* **443** (2014) L11.
216. S. R. Kulkarni, E. O. Ofek, J. D. Neill, Z. Zheng and M. Juric, *ApJ* **797** (2014) 70.
217. J. M. Cordes and I. Wasserman, *ArXiv e-prints/1501.00753* (2015).
218. M. Mannarelli, G. Pagliaroli, A. Parisi and L. Pilo, *Phys. Rev. D* **89** (2014) 103014.
219. A. Barrau, C. Rovelli and F. Vidotto, *Phys. Rev. D* **90** (2014) 127503.
220. Y.-W. Yu, K.-S. Cheng, G. Shiu and H. Tye, *J. of Cosm. & Astrop. Phys.* **11** (2014) 40.
221. Y. Lyubarsky, *MNRAS* **442** (2014) L9.
222. J.-P. Macquart, E. Keane, K. Grainge, M. McQuinn, R. P. Fender, J. Hessels, A. Deller, R. Bhat, R. Breton, S. Chatterjee, C. Law, D. Lorimer, E. O. Ofek, M. Pietka, L. Spitler, B. Stappers and C. Trott, *ArXiv/1501.07535* (2015).

Table 1. Selected aspects of fundamental physics studied with radio astronomical techniques compared to other methods. Note that some solar system tests have better numerical precision but are derived in weak gravitational field of the Solar System. In contrast, binary pulsar limits may sometimes be less constraining in precision, but they are derived for strongly self-gravitating bodies where deviations are expected to be larger. References are given for more information or further reading. For a general review see Will (2014), and for pulsar-related limits see Wex (2014).

Tested phenomena	Method	Radio astronomy	Ref.
Variation of fundamental constants:			
Fine structure constant (e^2/hc)	Clock comparison, radio active decays, limit depending on redshift, $< \sim 10^{-16} \text{ yr}^{-1}$	Quasar spectra, $< 10^{-16} \text{ yr}^{-1}$	135
e-p mass ratio	Clock comparison, $< 3.3 \times 10^{-15} \text{ yr}^{-1}$	Quasar spectra, $< 3 \times 10^{-15} \text{ yr}^{-1}$	136,137
Gravitational constant, \dot{G}/G	Lunar Laser Ranging (LLR), $(-0.7 \pm 3.8) \times 10^{-13} \text{ yr}^{-1}$	Binary pulsars, $(-0.6 \pm 3.2) \times 10^{-12} \text{ yr}^{-1}$	138, 139, 140
Universality of free fall:	LLR, Nordvedt parameter, $ \eta_N = (4.4 \pm 4.5) \times 10^{-4}$	Binary Pulsars, $\Delta < 5.6 \times 10^{-3}$	135, 141, 140
Universal preferred frame for gravity:		see Table 2	
PPN parameters and related phenomena:		see Table 2	
Gravitational wave properties:		Binary pulsars	140
Verification of GRs quadrupole formula		Double Pulsar, $< 3 \times 10^{-4}$	142
Constraints on dipolar radiation		PSR-WD systems, $(\alpha_A - \alpha_B)^2 < 4 \times 10^{-6}$	139, 143
Geodetic precession	Gravity Probe B, 0.3%	PSR B1913+16; Double Pulsar, 13%; PSR B1534+12, 17%	144, 145, 146
Equation-of-State	e.g. thermal emission from X-ray binaries	fast spinning pulsars; massive neutron stars	147, 17, 148, 143, 149
Cosmology	e.g. Supernova distances	CMB	this conference

Table 2. Best limits for the parameters in the PPN formalism. Note that 6 of the 9 independent PPN parameters are best constrained by radio astronomical techniques. Five of them are derived from pulsar observations. Adapted from Will (2014) but see also Wex (2014) for details.

Par.	Meaning	Method	Limit	Remark/Ref.
$\gamma - 1$	How much space-curvature produced by unit rest mass?	time delay	2.3×10^{-5}	Cassini tracking/135
		light deflection	2×10^{-4}	VLBI/135
$\beta - 1$	How much “non-linearity” in the superposition law for gravity?	perihelion shift	8×10^{-5}	using $J_{2\odot} = (2.2 \pm 0.1) \times 10^{-7}/135$
		Nordtvedt effect	2.3×10^{-4}	$\eta_N = 4\beta - \gamma - 3$ assumed/135
ξ	Preferred-location effects?	spin precession	4×10^{-9}	Isolated MSPs/150
α_1	Preferred-frame effects?	orbital polarisation	4×10^{-5}	PSR-WD, PSR J1738+0333/151
α_2		spin precession	2×10^{-9}	Using isolated MSPs/152
α_3		orbital polarisation	4×10^{-20}	Using ensemble of MSPs/141
ζ_1	Violation of conservation of total momentum?	Combining PPN bounds	2×10^{-2}	135
ζ_2		binary acceleration	4×10^{-5}	Using \ddot{P} for PSR B1913+16/135
ζ_3		Newton’s 3rd law	10^{-8}	lunar acceleration/135
ζ_4		not independent parameter		$6\zeta_4 = 3\alpha_3 + 2\zeta_1 3\zeta_3$

Table 3. Constraining specific (classes of) gravity theories using radio pulsars. See text and also Wex (2014) for more details.

Theory (class)	Method	Ref.
<u>Scalar-tensor gravity:</u>		
Jordan-Fierz-Brans-Dicke	limits by PSR J1738+0333 and PSR J0348+0432, comparable to best Solar system test (Cassini)	139 Freire priv. comm.
Quadratic scalar-tensor gravity	for $\beta_0 < -3$ and $\beta_0 > 0$ best limits from PSR-WD systems, in particular PSR J1738+0333 and PSR J0348+0432	139 Krieger et al. in prep., Freire priv. comm.
Massive Brans-Dicke	for $m_\varphi \sim 10^{-16}$ eV: PSR J1141–6545	153
<u>Vector-tensor gravity:</u>		
Einstein-Æther	combination of pulsars (PSR J1141–6545, PSR J0348+0432, PSR J0737–3039, PSR J1738+0333)	154
Hořava gravity	combination of pulsars (see above)	154
<u>TeV_S and TeV_S-like theories:</u>		
Bekensteins TeV _S	excluded using Double Pulsar	142
TeV _S -like theories	excluded using PSR 1738+0333	139

